CER-ETH – Center of Economic Research at ETH Zurich

Land Consolidation Reforms: A Natural Experiment on the Economic and Political Effects of Agricultural Mechanization

G. Loumeau

Working Paper 22/376
November 2022

Economics Working Paper Series

Eidgenössische Technische Hochschule Zürich
Swiss Federal Institute of Technology Zurich

Land Consolidation Reforms: A Natural Experiment on the Economic and Political Effects of Agricultural Mechanization

Gabriel Loumeau *

ETH Zurich

November 4, 2022

Abstract

This paper studies the causal economic and political effects of agricultural mechanization. For identification, it exploits a spatial discontinuity in the intensity of mechanization induced by land consolidation reforms in France between 1945 and 2008. The results suggest that an increase in mechanization leads to long-term growth in population (+9.5%), employment (+15%), and income (+0.5%), but also to an increase in the far-right vote share (+6.1%). To explain the rise in populism despite significant economic growth, the paper shows that mechanization also induces significant immigration flows and changes in social organization (via the decline of the family farm model).

Keywords: Mechanization, Natural experiment, Land consolidation, Local activity, Populism.

JEL classification: D72, O33, Q12, Q15, N54.

*Corresponding author: ETH Zurich, Department of Management, Technology, and Economics, Leonhardstrasse 21, 8092 Zurich, Switzerland; E-mail: loumeau@ethz.ch; +41 44 632 67 58.

1 Introduction

In the wake of World War II, agricultural production in the Western World experienced a rapid and large-scale mechanization. Between 1950 and 1959, the total number of agricultural tractors in Great-Britain, West-Germany, Italy, France, Belgium and Luxembourg increased from 360,000 to 1,800,000 units. Similarly, in the US, the number of tractors jumped from 1.5 million in 1940 to 4.7 millions in 1960. Agricultural mechanization differs from automation trends in manufacturing in that machinery did replace humans, but above all draft animals.[1] As illustration, in the six European countries mentioned, the number of horses and draft cows declined by 37.8% in just 10 years, between 1950 and 1959.[2] In the US, the number of horses and mules used in agriculture dropped from 15 million in 1940 to just 3 million in 1960. Despite the importance of this transformation, we have little empirical – and even less causal – evidence on the socio-economic effects of agricultural mechanization. How did mechanization impact population, employment and income growth in the short- and long-runs? Was voting behavior impacted? How was the agricultural society affected (e.g., in terms of female labor force participation, immigration or farm structure)?

To fill this gap, this paper studies the economic and political effects of agricultural mechanization using a natural experiment in France. When modern agricultural machines became available, traditional farms were overly fragmented for the efficient use of these machines. To remedy this problem, France – as many other countries – engaged in large-scale *land consolidation reforms*. By strategically trading parcels among farmers, such reforms generated longer and wider fields better suited for tractor and other machines, as illustrated in Figure 1.[3] In France, land consolidation reforms started in 1945, peaked around 1965 and continued at an ever slower rate until 2008. In the North-West of France, the intensity of land consolidation reforms – and consequently in the adoption of modern ma-

[1] As explained in the 1950 United States Census of Agriculture: "tractors are important because they combine added power with machinery that can do work that is not possible with horses or mules. [...] The power take-off increases the efficiency and dependability of harvesting equipment like mowers, combines, corn pickers, and sillage cutters." (United States. Bureau of the Census and United States. Bureau of Agricultural Economics, 1952)

[2] In Great-Britain, West-Germany, Italy, France, Belgium and Luxembourg, the number of horse (draft cows) declined from 3,9 million (3,7 million) in 1950 to only 2.8 million (2 million) in 1959. Comparatively, the agricultural worker share drop by 21.2% between 1930 and 1980, a period 5 times longer.

[3] Figure A1 presents a schematic representation of a land consolidation reform. In their vast majority, land consolidation reforms insured that farmers would not experience an increase or decrease in their total owned land. In the rare instances in which soil quality differed greatly within a municipality, consolidation reforms aimed to keep production capacity equal for each farmer.

chinery – exhibits a 800km long sharp spatial discontinuity following variation in geological characteristics between the Paris basin and the Central and Armorican Massifs. I use this discontinuity to set a spatial Regression Discontinuity (RD) design following Hahn, Todd, and Van der Klaauw (2001); Calonico, Cattaneo, and Titiunik (2014); Calonico, Cattaneo, and Farrell (2020) and estimate the causal effect of mechanization on local socio-economic outcomes. Concerning the treatment intensity, I estimate that by 2010 the annual value of agricultural production was €692 per ha larger on the border side with a higher rate of mechanization (i.e., towards the Paris basin).[4]

Figure 1: Aerial photographs before and after a land consolidation reform

Source: Screenshot from IGN's Geoportail (taken on 08/02/2022). Municipality is La Noe in Mayenne in France in 1949 and 2016. Schematic representation of a land consolidation reform is presented in Figure A1. Years 1949 and 2016 are chosen following data availability of aerial photographies over France's rural areas.

Using local polynomial regression-discontinuity estimations with robust bias-corrected confidence intervals, I find that an increase in mechanization leads to a long-term growth in population (+9.5%), employment (+15%), income (+0.5%) and female labor force participation (+0.3%), but also to an increase in the far-right vote share (+6.1%). Gains in the far-right vote share appear to come from lower far-left and center right votes shares, and not via a turnout effect.

To explain why the far-right vote share increases despite significant economic growth,

[4]The gain in productivity can also be expressed per agricultural worker. I then estimate a productivity jump of €6458 per worker and year.

I investigate two channels highlighted by the political economy literature on populism.[5] First, in line with previous findings (Barone, D'Ignazio, de Blasio, and Naticchioni, 2016; Halla, Wagner, and Zweimüller, 2017; Becker, Fetzer, and Novy, 2017; Dustmann, Vasiljeva, and Piil Damm, 2018), I estimate that higher mechanization is associated with higher immigration (+3 non-local workers per 100 residents, mostly with birthplace outside of France). Second, voters may view negatively the economic and social transformation of their localities as it changes core determinants of the local identity (Fukuyama, 2018; Noury and Roland, 2020). Using historical data from the French Agricultural census since 1970, I find that mechanization leads to a decline in the family farm model in favor of more professional and heavily mechanized structures. The feeling of "not recognizing" their municipality may then encourage reactionary sentiments in voters.

I conduct a series of complementary approaches to insure the robustness of the results. First, when sufficient historical data is available (e.g., for population, employment, migration, economic transformation, female labor force participation, etc), I confirm the RD results using a difference-in-differences design with staggered treatment adoption following Borusyak, Jaravel, and Spiess (2021). This approach has the advantage of directly controlling for possible differences in pre-trends. Second, I conduct a series of smoothness tests on all available time invariant covariates and covariates pre-1945. These include historical population density at the municipal level since 1876, municipal fundamentals (e.g., area, presence of a river, elevation), historical transport networks (from the roman empire, and the 18th century road network), as well as historical urbanization tests (number and size of 18th century settlements). All covariates vary smoothly around the threshold. Furthermore, I exploit the fact that soil composition was a strong determinant of the intensity of land consolidation to inform a fuzzy regression discontinuity design. Formally, I exploit the distance to the geological composition border as a first stage predictor for distance to the land consolidation border. Beyond validity tests (which are also conducted successfully), this allows me to tackle the endogenous border placement problem. Finally, I also propose a series of standard robustness tests, such as placebo tests when varying the placement of the border artificially or bandwidth tests varying the size of the bandwidth.

Contribution. This research is related to several strands of existing work. First, to my knowledge, this paper is the first natural experiment on agricultural mechanization, and the first causal estimation of mechanization in the developed world. This paper studies a wide range of outcomes (i.e., from farm productivity to voting behavior) in the short-, and

[5] Guriev and Papaioannou (2020) reviews the literature.

long-run. In a developing context, Pingali (2007) reviews the early agricultural mechanization literature. Recently, Caunedo and Kala (2021) study the causal effect of agricultural mechanization on labor supply, farm productivity and labor demand using a randomized control trial. Within the mechanization literature, the topic of land fragmentation and subsequent consolidation has also received attention in a wide variety of contexts: among others, in Europe (Vitikainen, 2014), in the US (MacDonald, Hoppe, and Newton, 2018; MacDonald, 2020), in China (Deininger, Jin, and Xia, 2012), and in India (Deininger, Monchuk, Nagarajan, and Singh, 2014).

As mechanization is a particular instance of automation, this paper contributes to the large literature on automation which has been shown to be a source of great labor market change, with consequent effects on voting behavior (see, among others, Goldin and Katz, 1998; Acemoglu and Autor, 2011; Autor and Dorn, 2013; Goos, Manning, and Salomons, 2014; Acemoglu and Restrepo, 2018; Graetz and Michaels, 2018; Acemoglu and Restrepo, 2019; Anelli, Colantone, and Stanig, 2021). Yet, the literature has mostly focused on automation in manufacturing. Mechanization – and thus, this paper – differs from automation in (at least) two aspects. First, in the mechanization process, machines replaced above all draft animals. Human labor is evidently also affected, but most likely in a smaller magnitude. Second, the initial economic structure, i.e., predominance of family farms, was very different. These important differences can induce mechanization to have largely different socio-economic effects than automation.

This paper also contributes to the literature studying mechanization and automation as a determinant of populism (Frey, Berger, and Chen, 2018; Bó, Finan, Folke, Persson, and Rickne, 2018; Im, Mayer, Palier, and Rovny, 2019; Dijkstra, Poelman, and Rodríguez-Pose, 2020; Anelli et al., 2021; Guriev and Papaioannou, 2020, review the literature). To the best of my knowledge, this paper is the first to study the causal relationship between mechanization and populism. This paper highlights the importance of immigration induced by mechanization to understand the rise in populism (Barone et al., 2016; Halla et al., 2017; Becker et al., 2017; Dustmann et al., 2018). Aside from immigration, this paper provides evidence that the perception of socio-economic transformations may also lead to an increase in the far-right vote share (in line with evidence in, e.g., Akkerman, 2015; Spierings and Zaslove, 2015; Graetz and Michaels, 2018; Dauth, Findeisen, Suedekum, and Woessner, 2018). Such socio-economic changes include the labor shift away from agriculture towards other sectors (despite significant labor growth), as well as a reaction to the departure from the traditional family farm structure.

Finally, this paper contributes to the historical discussion on land organization, productivity and economic growth (early discussions can be found in Samuelson, 1954; Marx, 1990). For instance, Heldring, Robinson, and Vollmer (2022) have recently shown that parliamentary enclosures in England between 1750 and 1830 have led to higher crop yields. In line with this result, this paper shows that a more efficient land organization – obtained via land consolidation – can lead to significant gains in productivity, which in turn affects population, employment and local income growth.

The reminder of this paper is organized as follows. Section 2 presents the historical and technological background motivating the land consolidation reforms in France after 1945. Before presenting the empirical approach, validity tests and the main results in Section 4, I described the various datasets used in this paper in Section 3. Then, Sections 5, 6 and 7 discuss the results on local economic activity, voting behavior and societal outcomes, respectively. Finally, Section 8 concludes.

2 Background

2.1 Mechanised agriculture and land consolidation in France after 1945

Following World War II, the arrival of modern farming machines – such as combined harvesters – promised large productivity gains in agriculture. Yet, the historical fragmented field organization in rural areas was ill-suited for the use of modern machines. Traditionally, farmers owned and grew crops on spatially disconnected fields, whereas modern mechanised techniques are most productive in large continuous fields. As a remedy, large scale land consolidation reforms took place in most developed countries. Such reforms allowed farmers to trade off equally sized (and productive) pieces of land to create larger contiguous fields more suited for mechanization.

The impact of land consolidation on mechanization did not take long to materialize. The French fleet of tractors grew from 37,000 in 1945 to 830,000 units in 1962. The increase is even greater when looking at the growth of combine harvesters' fleet from just 250 in 1945 to 67,000 in 1962. Taking a more global look, between 1950 and 1959, the total number of agricultural tractors in Great-Britain, West-Germany, Italy, France, Belgium and Luxembourg increased from 360,000 to 1,800,000 units. At the same time, the numbers of draft animals has greatly declined. In these six countries, the number of horses decreased from 3,900,000 in 1950 to 2,800,000 in 1959; whereas the number of draft cows declined from

Figure 2: NUMBER OF CONSOLIDATED MUNICIPALITIES IN FRANCE (1945-2010)

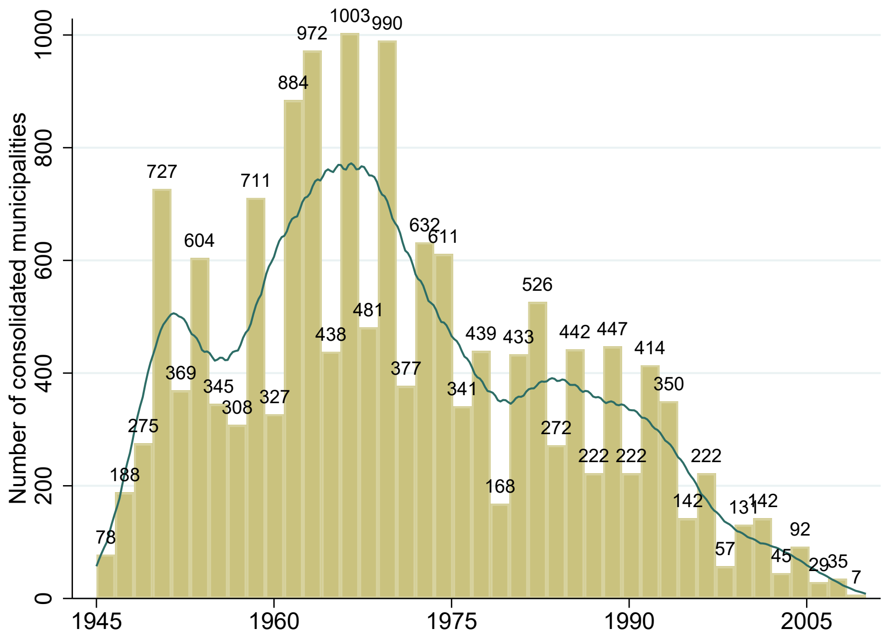

Source: Author's own illustration based on the land consolidation database by Philippe and Polombo (2013). By 2010, out of 36,766 municipalities in France, 15,498 (i.e., 42%) had consolidated their agricultural land.

3,700,000 in 1950 to only 2,000,000 in 1959.[6]

By 2010, out of 36,766 municipalities in France, 15,498 (i.e., 42%) had consolidated their agricultural land.[7] Figure 2 shows the number of consolidated municipalities between 1945 and 2010 based on the land consolidation database by Philippe and Polombo (2013). The reforms started rapidly after 1945 to peak in the mid-1960s before slowly decreasing until 2008. Figure A2 illustrates the location of the land consolidation reforms over time.

Figure 1 illustrates the typical transformation of farmland organization before and after land consolidation using aerial photographs in 1949 and 2016 over the French department of *Mayenne*. The 1949 photograph (left) reveals multiple divided fields separated by many hedgerows. Almost 70 years later, fields are larger and much less divided, as revealed in the 2016 photograph (right). Two key benefits of land consolidation appear clearly: first, continuous fields are much longer and wider (hence, better suited for large modern machines); second, the commuting requirements across fields is reduced. Figure A1 shows the outcome of a consolidation reform in a schematic manner.

[6] *Source*: Le Monde, March 5th, 1963.

[7] This share would likely rise significantly if excluding urban municipalities who do not have any agricultural land to consolidate.

2.2 Soil composition and land consolidation

The density of local land consolidation reforms was not uniform across France. Municipalities in the Paris basin typically engaged heavily into land consolidation. The intensity of consolidation in the basin is the consequence of a particularly attractive soil for crops: silty soil. Figure A3 illustrates the various types of soil in metropolitan France. Silty soil is usually more fertile than other types of soil, as silt promotes water retention and air circulation. In the Paris basin, the *Beauce* region south of Paris between the Seine and the Loire is a typical example of an highly productive agricultural area, traditionally named "the granary of France". As illustrated in Figure A3, the soil composition changes rapidly when moving West (towards Brittany) and South (towards the Central Massif) as soil becomes poorly differentiated unaltered soils. This type of soil is much less productive for agricultural purposes. Importantly, elevation increases as one moves towards the Massifs, but it varies smoothly in space.[8] Figure A3 also shows the location of the *Seuil du Poitou*, a narrow corridor (about 50km) south of the Armorican massif and West of the Central massif with silty soil. This corridor is used for several robustness tests in Sections 5 and 6.

Due to the variation in soil composition which imply different yield, the intensity of land consolidation reforms is much smaller in municipalities away from the Paris basin. To measure this intensity – in line with the aerial picture in Figure 1 – geographers and agricultural scientists commonly use the density of hedgerow. As opposed to other metric, such as the municipal area of consolidated land, the reduction in hedgerow density is a very accurate indicator of the suitability of post-consolidated fields to modern machinery. Hence, using the National Institute of Geographic and Forest Information's BDTOPO layer (2021), I computed the density of hedgerow (in m/ha) across municipalities.

To illustrate the spatial variation in hedgerow density, I highlight in Figure 3a municipalities with low density (i.e., 35m/ha or less) in yellow, and high density (i.e., more than 35m/ha) in green. Clearly, a (rather) well define border splits the area in two. As a reference point, Figure 3 also shows the location and size of Paris metropolitan area in grey. Using high-resolution spatial data, Figure 3b shows a zoom on the actual geo-referenced hedgerows in the area delineated by the red rectangle in Figure 3a. A clear reduction in hedgerow density appears as one moves East.

To move away from an arbitrarily chosen density threshold and accurately delineate the intensely consolidated area in the Paris basin, I group municipalities based on their density of hedgerow in m/ha using k-means clustering (Hartigan and Wong, 1979; Alpaydin,

[8] The validity tests in Table A3 shows that average elevation and within-municipality standard deviation in elevation evolves smoothly around the spatial discontinuity studied.

Figure 3: Measuring the intensity of land consolidation using hedgerow density

(a) Municipal hedgerow density (m/ha) and the k-means border

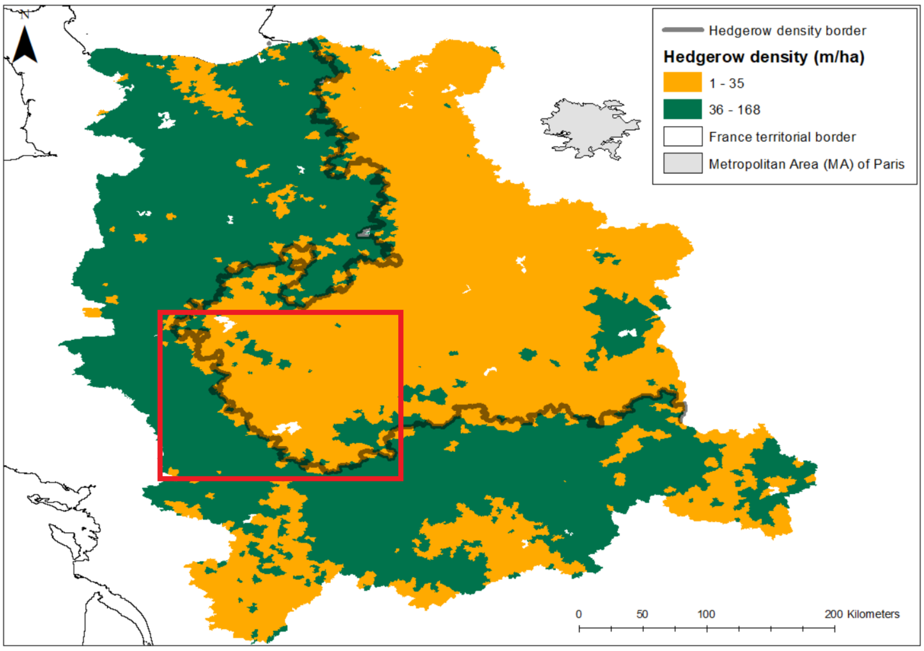

(b) Zoom on actual hedgerows around the k-means border

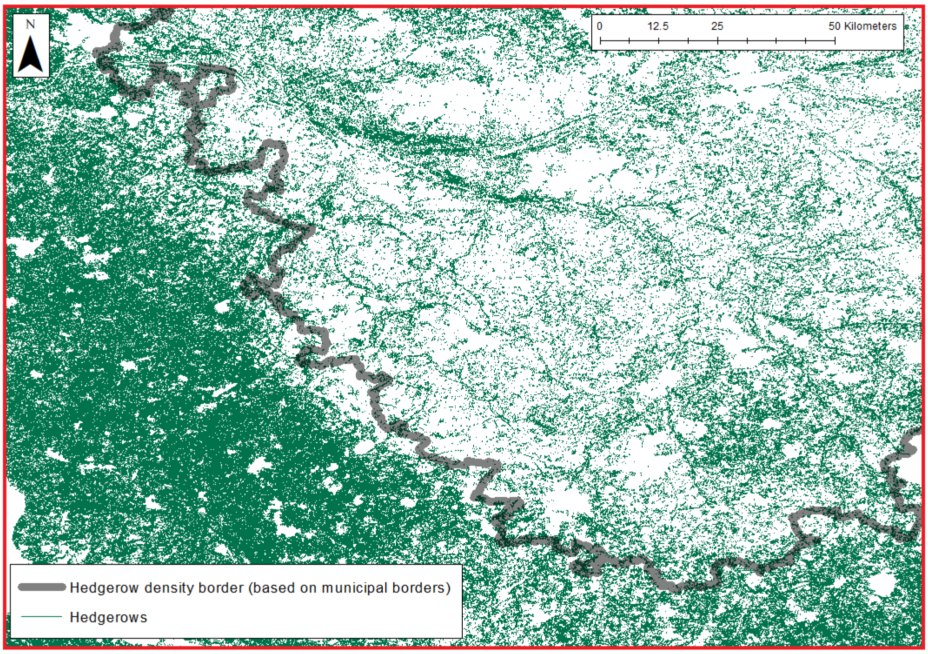

Notes: Figure 3b is a zoom on the area delineated by the red rectangle in Figure 3a. *Source:* Inra, BDGSF, Ministry of Ecology, Sustainable Development and Energy. Author's own translation. *Scale:* 1/1 000 000, 1998. *Processing*: SOeS, 2014.

2020). This standard Machine Learning approach proceeds by defining groups such that the variance within each group is minimized. Formally, the method solves the following problem:

$$\arg\min_{\theta} \sum_{i=1}^{k} \sum_{\boldsymbol{x} \in S_i} ||\boldsymbol{x} - \boldsymbol{\mu}_i||^2 \tag{1}$$

where $k = 2$ is the number of clusters, $\boldsymbol{x}$ is the municipal density of hedgerow and $\boldsymbol{\mu}_i$ is the mean of points in S_i. The resulting border is highlighted in black in Figure 3a and 3b.

2.3 Resulting spatial discontinuities

To insure that the hedgerow density does vary discontinuously between the two zones in Figure 3, I use a data-driven regression-discontinuity plot following Calonico et al. (2014). This permits testing whether the share of consolidated land and local hedgerow density vary discontinuously at the cluster border mapped in Figure 3.

Figure 4 presents the results focusing on the share of consolidated land in the total area of a municipality (Panel a), and on the average hedgerow density within a municipality (Panel b). Municipalities in the Paris basin (i.e., East of the border) are attributed positive distances to the cluster border, whereas distance to the border on the other side increases negatively. An highly significant discontinuity is observed at the border for both variables. Municipalities in the Paris basin (i.e., with silty soils) have a discontinuously higher share of consolidated land (gap of about 19 percentage points), and an associated significantly lower hedgerow density (gap of 30m/ha).[9]

3 Data

I draw on various sources of geo-localized and historical data. All data used are freely available. In what follows, I briefly describe the key databases used in this paper. Descriptive statistics are reported in Tables A1 (municipal level) and A2 (200m2 cells level).

Land consolidation. Land consolidation information is extracted from the land consolidation database by Philippe and Polombo (2013). It covers the period 1945-2010. Among others variables, the database includes the size and year of consolidation reforms for each consolidated municipality. To measure precisely the impact of the consolidation reforms, I also use geo-localized information on hedgerow location and length provided

[9] In Section 4, I run placebo tests where I study how the discontinuities observed in Figure 4 vary if moving the cluster border by ±1km. Figure A10 reveals that the cluster border corresponds indeed to a spatial discontinuity, and is ideally placed as moving the border by "only" 1km Westward or Eastward leads to much less strict discontinuities.

Figure 4: Spatial discontinuities in land consolidation

(a) Share of consolidated land

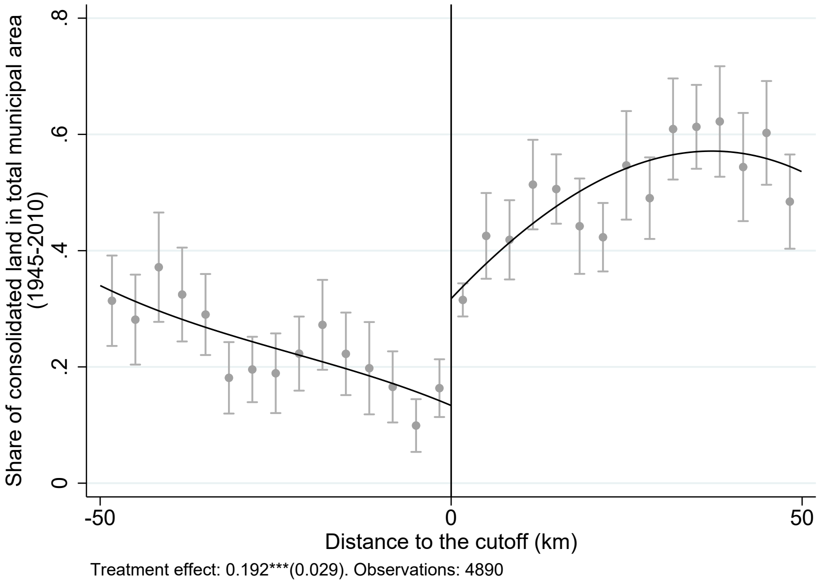

(b) Hedgerow density (in m/ha)

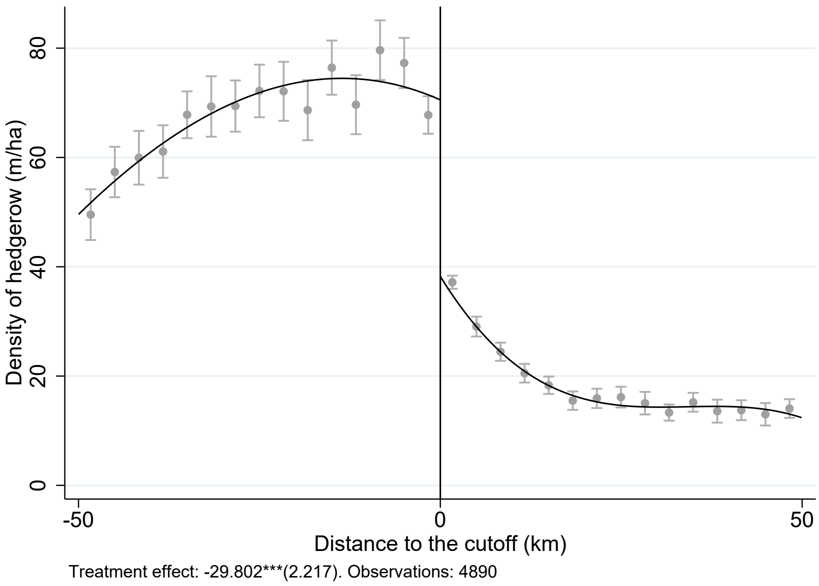

Notes: Data-driven regression-discontinuity plot following Calonico et al. (2014). Figure also reports the treatment effect based on local polynomial regression-discontinuity estimation with robust bias-corrected confidence intervals. *Source Panel a:* Consolidated area within each municipality is computed using the land consolidation database by Philippe and Polombo (2013). *Source Panel b:* Hedgerow data is extracted from the French National Institute of Geographic and Forest Information's BDTOPO layer (2021).

by the French National Institute of Geographic and Forest Information's BD TOPO layer (https://geoservices.ign.fr/documentation/donnees/vecteur/bdtopo).[10]

Electoral data. All voting data is provided by the French centralized public data platform: https://www.data.gouv.fr/fr/. The election data used in this paper is recorded at the municipality level. To study voting behavior in an homogeneous context over space and time, I primarily focus on the first round of the presidential elections in 2002, 2007, 2012 and 2017. Between 1965 and 2002, the electoral data on presidential elections is only available at the departmental level. Consequently, to study the evolution of voting behavior in the long-run (1965-2017), I focus on departmental vote share averages.

Soil composition. The map of the soil composition of France presented in Figure A3 is produced by the French Ministry of Ecology, Sustainable Development and Energy. To perform formal quantitative test around the exact soil border, I geo-referenced the border using GIS tools.

Agricultural censuses since 1970. To understand how mechanization impacted the worker structure of French farms, I use all vintages of the French Agricultural Census since 1970 (https://agreste.agriculture.gouv.fr/agreste-web/). Produced every (approximately) ten years by the French Ministry of Agriculture, the agricultural census aims to produce a complete picture of the French agricultural world. It covers the years: 1970, 1979, 1888, 2000 and 2010. I extracted information for every vintage on the number of agricultural workers in each municipality, as well as their role in the farm, i.e., whether a worker is the head of the farm, a spouse working in the farm, or a family members working in the farm. The 2010 Agricultural census also includes information on productivity per ha and per workers, which I use to compute the long-term productivity effect of mechanization.

Municipal population count since 1876. The municipal population count at regular (approximately 10 years) intervals since 1876 is made available by the The National Institute of Statistics and Economic Studies (INSEE).

Workplace employment by municipality since 1968. The National Institute of Statistics and Economic Studies offers harmonized censuses on the structure of the ac-

[10]The BD TOPO is a 3D vector description of the elements of the territory and its infrastructures, with metric precision, usable at a scale of 1:2000. It coherently covers all the geographical and administrative entities of the national territory.

tive population (aged 25 to 54) since 1968 at the municipal level. For each municipality, the number of workers by sector of activity and gender is provided. In particular, this database allows me to follow the share of agricultural workers since 1968 at a 7 to 10 year interval.

Geo-localized data. To study variation in population and income at very fine spatial resolution, I use the 2015 "données carroyées à 200m^2 sur la population" (lit. gridded population data at 200m^2). These data contain the population count, the number of households below the poverty line, and the sum of individual incomes for the individuals residing in a 200m^2 cell.[11]

Geo-localized 18th century Cassini map. Geo-localized information on the historical structure of urban cities is obtained from the 18th century Cassini roads and cities dataset (Harvard Dataverse, Perret, Gribaudi, Barthelemy, Abadie, Baciocchi, Bertelli, Bonin, Bordin, Costes, Cristofoli, Dumenieu, Gravier, Hubert, Le Ny, Mermet, Motte, Pardoen, Raimond, Robert, and Vouloir, 2015). The database represents the urban network at the French national level described in the historical map of Cassini in the 18th century, which is the first topographic and geometric map established of the Kingdom of France as a whole.

Miscellaneous. Finally, I also collected standard municipality level information from the National Institute of Statistics and Economic Studies on local socio-economic outcomes, such as local demography, migration and public finance.

4 Empirical strategy

4.1 Spatial Regression Disconstinuity (RD) Design

Consider $i \in I$ local areas, each is spatially defined by its centroid, $\boldsymbol{c}_i = (c_i^x, c_i^y)$. In the present setting, areas alternatively represent municipalities or 200m2 grid cells. Further, consider $\overline{\boldsymbol{B}}$ as the infinite set of border points constituting the mechanization border. I then define the subset $\boldsymbol{B} \in \overline{\boldsymbol{B}}$ of border points $\boldsymbol{b}_i = (b_i^x, b_i^y)$, such that the euclidean distance to the mechanization border $d_i = ||\boldsymbol{c}_i - \boldsymbol{b}_i||$ is minimized. Finally, define two zones $\mathcal{A}^+$ and $\mathcal{A}^-$ as the treatment (i.e., higher level of mechanization, towards the Paris basin) and

[11] To respect individual data confidentiality, individual incomes are winsorized the 5th and 95th percentiles of the departmental (NUTS3) individual income distribution.

the control (i.e., lower level of mechanization, towards the Armorican and Central Massifs) areas, respectively.

Distance to the nearest mechanization border point acts as the forcing variable. Assignment into treatment is then a function of a municipality's location relative to the border. Formally, treatment status T_i of municipality i is defined as $T_i = \mathbb{1}\left[\boldsymbol{c}_i \in \mathcal{A}^+\right]$. Denote the outcome vector by $\boldsymbol{Y}$. I then focus on the discontinuity of the expected outcomes at the geographical border:

$$\tau(\boldsymbol{d}) \equiv \mathbb{E}[\boldsymbol{Y}_1 - \boldsymbol{Y}_0 | d_i = 0] = \lim_{\boldsymbol{d} \to 0}[\boldsymbol{Y} | \boldsymbol{c} \in \mathcal{A}^+] - \lim_{\boldsymbol{d} \to 0}[\boldsymbol{Y} | \boldsymbol{c} \in \mathcal{A}^-]. \tag{2}$$

As baseline specification, I estimate (2) using local-polynomial regression-discontinuities with robust confidence intervals and optimal bandwidth selection following Calonico et al. (2014). The performance of standard local polynomial estimators may be seriously limited by their sensitivity to the specific bandwidth employed. Hence, I employ mean squared error optimal bandwidths, which are valid given the robust approach in Calonico et al. (2014). When including covariates, I follow the approach in Calonico, Cattaneo, Farrell, and Titiunik (2019).

Validity. A key requirement of a valid RD approach is that covariates vary smoothly around the threshold. To test this assumption, I conduct balancing tests around the discontinuity studied in the form of local polynomial regression-discontinuity estimations. I focus on time invariant and historical (pre-1945) variables. Table A3 reports the results. Panels (a) to (l) focus on population density at regular intervals (7 to 10 years) between 1876 and 1936. Panels (m), (n), (o) and (p) study municipal fundamentals such as the area, the presence of a river flowing through, municipal average elevation, and the municipal standard deviation in elevation. Panels (q) and (r) look at the presence of a roman road (ca. 117AD) and a main road in the 18th century, respectively. Finally, Panels (s) and (t) study the historical urban context around the threshold. Using the Cassini map, Panel (s) test for a discontinuity in the presence of an urban settlement during the 18th century, whereas Panel (t) focuses on the area of such settlements. No significant discontinuity is observed in the mentioned dimensions.

From land consolidation to productivity. Historical measures of land productivity at the municipal level are not available. Yet, to insure that the land consolidation reforms did lead to productivity gains – as shown in the literature (Deininger et al., 2012, 2014; Vitikainen, 2014; MacDonald et al., 2018; MacDonald, 2020) – I estimate the long-term productivity effect of land consolidation. To measure productivity at the municipal level, I use the 2010 vintage of the French agricultural census which records the production per ha and per worker. Using a local polynomial regression-discontinuity approach á la Calonico et al. (2014), Table 1 reveals that the annual value of agricultural production was €692 per ha and €6,458 per worker larger in the Paris basin's side of the border. This finding is confirmed by RD plots in Figure A6.

Table 1: MECHANIZATION AND LONG-TERM LAND PRODUCTIVITY

	(1)	(2)	(3)	(4)
	Production per ha (€)		Production per worker (€)	
Treatment effect	433.710**	692.299***	6075.620*	6458.101*
	(219.101)	(212.423)	(3578.599)	(3615.533)
Obs.	4,403	4,403	4,403	4,403
Bandwidth (km)	20.9	20.9	21.7	21.7
Obs. bw.	1,769	1,769	1,806	1,806
Department FE	Yes	Yes	Yes	Yes
Covariates	No	Yes	No	Yes
Bandwidth	Opt	Opt	Opt	Opt
Mean dep. var.	2169.8		107126.7	

Notes: Table reports local polynomial regression-discontinuity estimation with robust bias-corrected confidence intervals and inference procedures following Calonico et al. (2014). Data used from the 2010 vintage of the French National Agricultural Census.

Placebo test. In the present application, the exact placement of the threshold was not given as is normally the case with RD designs. Instead, the exact placement of the threshold was determined using k-means clustering. In Figure A10, I test whether the derived threshold does capture the location of the "true" threshold. Formally, I shift East-/Westward by 1km the threshold and non-parametrically study the share of consolidated municipal land on both sides. A close inspection of the outcome around the border reveals that shifting the threshold by $\pm$1km leads to a much less clean cut division; thus, validating the k-means approach.

4.2 Alternative identification strategies

Difference-in-Differences (DiD) with staggered treatment adoption. As shown in the validity paragraph above, a wide array of historical and time invariant variables vary smoothly around the threshold. Yet, one can never exhaust the full list of variables that would be required to fully validate a RD framework. Hence, as alternative identification strategy, I adopt a difference-in-differences design with staggered treatment adoption following Borusyak et al. (2021). This approach offers the key advantage of being able to test directly for differences in pre-trends. Even though the treatment and control groups may be less similar than in a RD framework, parallel pre-trends support the idea of a similar evolution across groups if the treatment would have never happened. Given that the majority of non-urban municipalities have been consolidated between 1945 and 2008 (but not all at the same time), an approach exploiting the staggered adoption of land consolidation for identification purposes appears well-suited.

Formally, I estimate the causal effect of a binary treatment D_{it} on outcome Y_{it} in a panel of units i and periods t. For each unit there is an event date E_i when D_{it} switches from 0 and 1 and stays there forever: $D_{it} = \mathbf{1}[K_{it} \geq 0]$, where $K_{it} = t - E_i$ is the number of periods since the event date. Given that historical census vintages are distant by 7 to 10 years, I assess the parallel behavior of the pre-trends using two time periods prior to treatment. Naturally, this identification strategy can only be applied for outcomes with sufficient historical data availability.

Fuzzy regression discontinuity design. To account for the fact that the exact placement of the mechanization border may not be random, I adopt a fuzzy regression discontinuity design as robustness identification strategy. Formally, I exploit the distance to the geological soil composition border (cf. Figure A3) as a first stage predictor for distance to the land consolidation border. Empirically, the distance to the geological composition border is revealed to be a strong predictor of the running variable (cf. Tables 2 and 6).

5 Effect on economic activity

To estimate the economic effects of agricultural mechanization on economic activity, I proceed in four steps. First, I focus on the impact of mechanization on population and employment. Then, I investigate the evolution of income and income inequality, before turning to the impact of mechanization on the local economic structure and on female labor force participation.

5.1 Mechanization, population and employment

Spatial RDD results. Table 2 reports the long-run effects of mechanization on population and employment. Column (1) reports results on the population density using gridded data at 200m2 in 2015, columns (2) and (3) on population density at the municipal level in 2010, columns (4) and (5) on the 2010 population growth measured relative to the 1936 municipal population, and columns (6) and (7) on municipal employment density *at the workplace*. Within the last three pairs, the second column includes covariates whereas the first does not. In each case, I report the total number of observations, the bandwidth used, the number of observations within the bandwidth, and the average of each outcome. Panel (a) reports estimates using the standard RD approach, whereas panel (b) presents results using the fuzzy discontinuity design introduced in Section 4. To capture the strength of the first stage, Panel (b) also reports the first stage estimates.

Overall, agricultural mechanization has a positive effect on population, independently of the metric used. As key figure, the fuzzy approach shows that population density was larger by 7 resident per km2 gap in 2010 on the more mechanized side of the border (column 3), which corresponds to a 9.5% increase relative to the population density within the optimal bandwidth. The magnitude difference between the standard and the fuzzy RD approach highlights the importance of controlling for possible strategic border placement. Mechanization also leads to an increase in employment. By 2010, municipalities on the more mechanized side hosted 3 workers more per km2. Given an average employment density within the optimal bandwidth of 18.9 workers per km2, the estimated effect represent a 15% growth in local employment density.

Figure 5 confirms the results in Table 2 by way of an RD plot. Population density at the 200m2 cell level is used as outcome. The optimal bandwidth of 6.19km is used. Given the high-resolution of the data, I use 30 equal sized bins on both sides. A clear discontinuous increase in population density is observed at the mechanization border. A similar RD plot for employment density at the municipal level is presented in Figure A7.

Results using difference-in-differences. The validity of the RD results relies on the assumption that – prior to consolidation reforms – all covariates on both sides of the border were smooth. The balance tests in presented in Table A3 support that claim, yet the magnitude difference between the standard and fuzzy RD approaches recommends a more cautious analysis. To insure that the observed results are not driven by prior differences around the border, I study the evolution of population and employment using a difference-in-differences design with staggered treatment adoption following Borusyak et al. (2021).

Table 2: Spatial RDD: Mechanization, population and employment

	(1)	(2)	(3)	(4)	(5)	(6)	(7)
	Gridded data	Municipal data					
	Pop. density (per km2)	Pop. density (per km2)		Pop. growth (%) (%)		Employment density (per km2)	
	(a) Sharp RD design						
Treatment effect	62.718***	36.970***	38.126***	21.957***	23.790***	13.954***	14.214***
	(4.902)	(10.728)	(10.696)	(7.607)	(7.503)	(4.588)	(4.581)
Obs.	208,739	4,747	4,747	4,747	4,747	4,888	4,888
Bandwidth (km)	6.19	29.1	29.1	29.1	29.1	28.8	28.8
Obs. bw.	17,489	2,285	2,285	2,285	2,285	2,341	2,341
	(b) Fuzzy RD design						
Treatment effect	12.793***	6.377***	7.215***	3.787**	4.502***	2.407***	2.697***
	(0.793)	(2.191)	(2.480)	(1.526)	(1.712)	(0.891)	(0.998)
Dist. soil border	3.991***	5.798***	5.284***	5.798***	5.284***	5.797***	5.271***
(1st stage)	(0.138)	(0.942)	(0.944)	(0.942)	(0.944)	(0.923)	(0.931)
Obs.	208,739	4,747	4,747	4,747	4,747	4,888	4,888
Bandwidth (km)	30*	29.1	29.1	29.1	29.1	28.8	28.8
Obs. bw.	75,380	2,285	2,285	2,285	2,285	2,341	2,341
Department FE	Yes	Yes	Yes	Yes	Yes	Yes	Yes
Covariates	No	No	Yes	No	Yes	No	Yes
Bandwidth	Opt	Opt	Opt	Opt	Opt	Opt	Opt
Mean dep. var.	16.024	73.871		33.259		18.848	

Notes: Table reports local polynomial regression-discontinuity estimation with robust bias-corrected confidence intervals and inference procedures following Calonico et al. (2014). Formal robustness test to bandwidth choice is presented in Figure A11. *: When estimating the fuzzy rdd with 200m2 cell data, I use a bandwidth of 30km to insure that the soil border lies within the data for all border points. Population growth is measured in percent between 1936 and 2010. Mean of dependent variable is computed using the optimal bandwidth.

Results are presented in Table A5. At regular 7 to 10 year intervals, municipal population is observed between 1876 and 2015, whereas municipal employment is observed between 1968 and 2015. For this analysis, I use the sample of all French municipalities as identification does not rely on proximity to the mechanization border. To control for pre-trends, I use two time periods (i.e., corresponding to approx. 15 years). The results are in line with the estimates in Table 2. Municipal population and employment increase following land consolidation. Moreover, I find that the ratio of employment to population for treated municipalities increases significantly following consolidation. This indicates that treated municipalities transformed to more dense employment centers. Interestingly, both population and employment decrease in the first pre-treatment period, even though in smaller magnitude than the later increase. This pattern can be interpreted as a first evidence of possible local economic transformation, where traditional agricultural jobs got

Figure 5: RD plot: Mechanization and population density

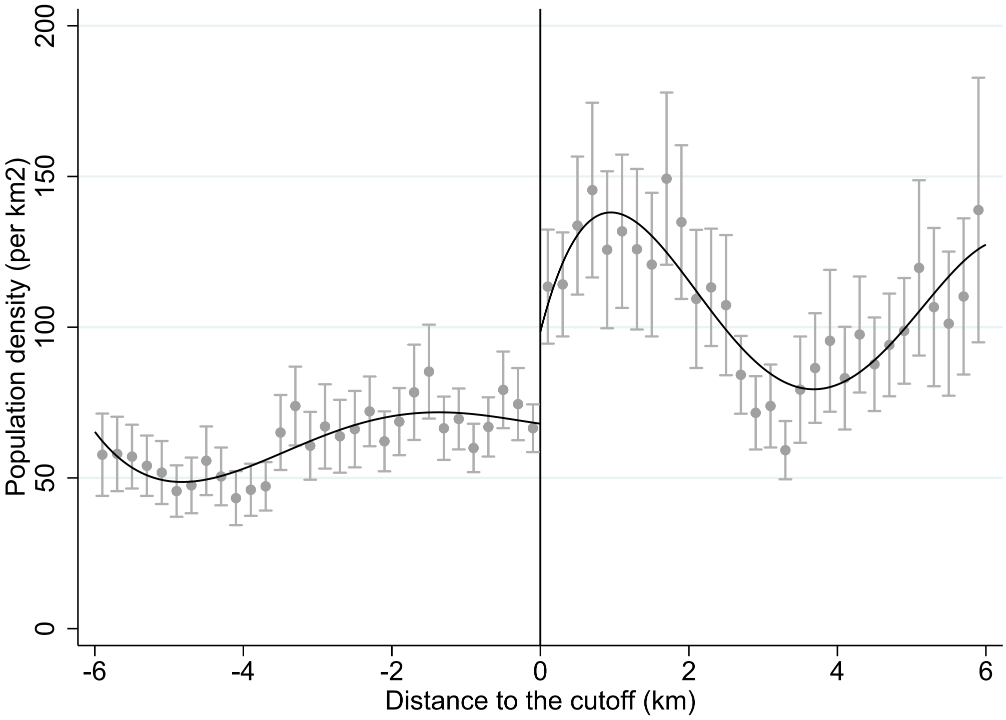

Notes: Data-driven regression-discontinuity plot following Calonico et al. (2014). 95% confidence intervals are presented. Outcome is the population density (per km2) by 200m2 cells.

replaced by skilled jobs in para-agriculture and manufacturing. I investigate this channel more thoroughly below.

Population differential over time (1876-2015). An alternative way to illustrate the impact of mechanization on population over time is to estimate the size of the population gap for each census vintage separately between 1876 and 2015. Results of this approach are presented in Figure A8. The municipal population for each year is the outcome. As a reminder, the figure highlights that the land consolidation reforms took place between 1945 and 2008 (cf. Figure 2). I find that the gap increases significantly in 1954 – and continuously until 1975 – which matches the most intense land consolidation period. After land consolidation reforms stopped in 2008, I observe the population gap to stabilize with a significantly higher level on the side of the Paris basin, i.e., more mechanized side.

Robustness using the *Seuil du Poitou*. To insure that the observed effects on population and employment are initially driven by underground soil quality (which determines consolidation reforms and subsequent mechanization), and not by other fundamental regional characteristics, I exploit the natural feature known as the *Seuil du Poitou*. Whereas a clear difference in soil composition and subsequent consolidation reforms is observed North (towards the Armorican massif) and East (towards the Central massif) of the area studied, the *Seuil du Poitou* (located between both massifs) does not exhibit such discontinuities. Hence, it offers a unique setting to insure that the observed patterns are not related to regional characteristics (e.g., distance to the Paris basin). In Tables A6 and A7, I replicate the approach in Table 2 but focusing only on the sub-sample of municipalities located on the *Seuil du Poitou*.[12] As expected, no long-term discontinuity is observed in this region in population (count, growth and density) or employment (count and density).

Robustness using placebo border shifts. To insure that the discontinuity in population and employment does take place at the mechanization border, I present placebo tests for population density and employment density in Tables A9 and A10, respectively. The tests consists in shifting the threshold spatially by $\pm$5km, $\pm$7km, $\pm$15km and $\pm$30km. The test confirms that the discontinuity in both outcomes is observed solely at the mechanization border. The magnitude of the estimated coefficient is closer to 0 for all placebo borders.

Robustness using alternative bandwidth sizes. Whenever estimating a RD design, I employ the optimal bandwidth selection criteria proposed by Calonico et al. (2014). Despite the clear advantages of using such bandwidth, it appears useful to investigate how sensitive are the results to the bandwidth size. Figures A11 and A12 presents a series of local polynomial regression-discontinuity estimation where the bandwidth size varies from half the optimal bandwidth to twice the optimal bandwidth, with 0.25 increments for population and employment density, respectively. Overall, the bandwidth size appears to have little effect on the results.

5.2 Mechanization and income

Following work on the relationship between automation, income and inequality (see, e.g., Acemoglu and Restrepo, 2021), I study how mechanization impacted long-run income and inequality. Formally, I estimate a RD design on income metrics around the mechanization border using both 200m2 cells and municipalities as units of analysis. The results are presented in Table 3. Column (1) to (4) focus on gridded data, whereas columns (5) and (6) use municipal data. Columns (1) and (2) report results for the total winsorized income (in log € per year) of residents of the cell, columns (3) and (4) analyse the fraction of households

[12] Formally, these are the municipalities in the NUTS3 region *Vienne*.

below the poverty line, and columns (5) and (6) look at the municipal median household income (in € per year). Within each pair, the first column reports results from the standard RD approach, whereas the second reports results from the fuzzy RD design.

Overall, I find that both the total income of the cell residents and the municipal median income are significantly larger on the more mechanized border side. As key figure, the yearly median household income is €99 larger, which is equivalent to a 0.5% increase relative to the average (column 6). This income effect supports the welfare improvement findings due to agricultural mechanization as reported in Caunedo and Kala (2021).

Studying inequality at the municipal level in (mostly) rural areas is difficult due to data confidentiality constraints. In France, distributional indexes are only available for municipalities with at least 2,000 residents, which is larger than the residential count of most municipalities around the border (average residential count is 1486 in 2010). Yet, the gridded data reports the fraction of poor households per capita within each 200m2 cells. Using this metric to study how mechanization affects the poorest households, the results are ambiguous. Using the RD specification, I do not find any significant effect on the fraction of poor households per capita, whereas the fuzzy RD speficication reports a significant – albeit of small magnitude – reduction in that number.

Table 3: Mechanization and income

	(1)	(2)	(3)	(4)	(5)	(6)
	Gridded data (200m2)				Municipal data	
	Total winsorized income (log(€/year))		Fraction of poor households (pc)		Median household income (€/year)	
	RD	Fuzzy RD	RD	Fuzzy RD	RD	Fuzzy RD
Treatment effect	0.266***	0.087***	<0.001	-0.003***	627.495**	99.270***
	(0.037)	(0.006)	(0.002)	(0.000)	(268.317)	(32.140)
Obs.	208,739	208,739	208,739	208,739	2,002	2,002
Bandwidth (km)	7.32	30*	9.25	30*	15.4	30
Obs. bw.	20,053	75,380	24,466	75,380	585	958
Mean dep. var.	11.604		0.107		16558.5	

Notes: Table reports local polynomial regression-discontinuity estimation with robust bias-corrected confidence intervals and inference procedures following Calonico et al. (2014). France's gridded population database at the 200m2 level is used. Income by 200m2 cells is winsorized at the 5th and 95th percentiles. Households are defined as poor if their income per consumption unit is below the administratively defined poverty line. *: When estimating the fuzzy rdd with 200m2 cell data, I use a bandwidth of 30km to insure that the soil border lies within the data for all border points. Mean of dependent variable is computed using the optimal bandwidth.

The results in Table 3 are graphically confirmed in Figure 6 by way of RD plot. Using the (log) total income within 200m2 cells, a clear discontinuity appears at the mechanization border.

Figure 6: RD plot: Mechanization and income

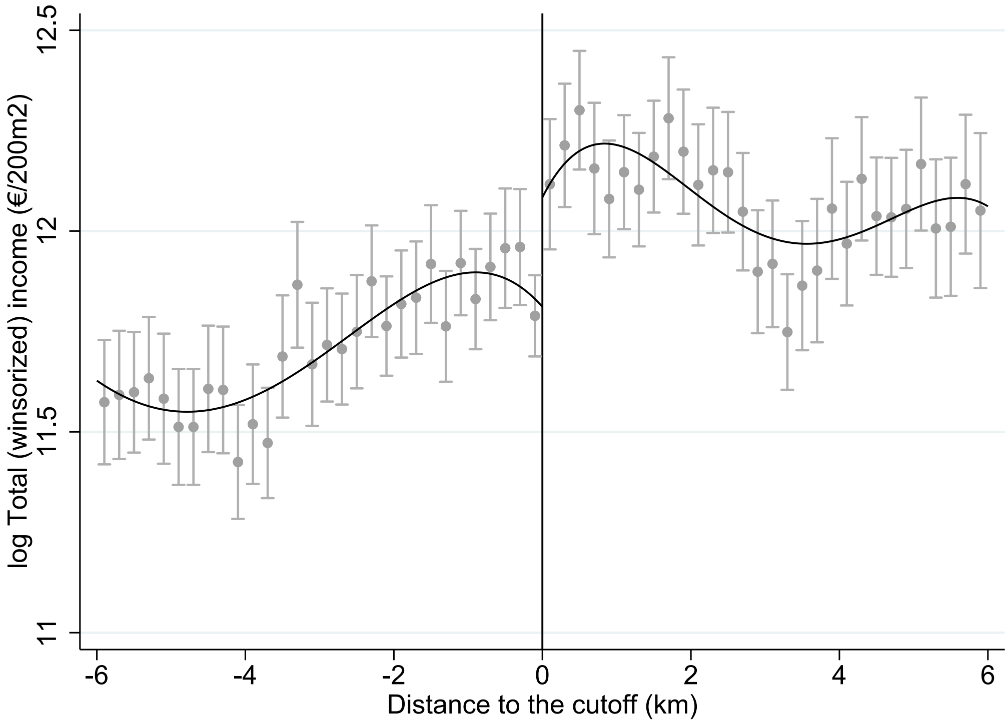

Notes: Data-driven regression-discontinuity plot following Calonico et al. (2014). 95% confidence intervals are presented. Income by 200m2 cells is winsorized at the 5th and 95th percentiles. Outcome is expressed in logs.

5.3 Local economic transformation

Thanks to historical labor data (at the workplace) availability, Table 4 studies the effect of agricultural mechanization on local labor shares by economic sectors using a difference-in-differences design following Borusyak et al. (2021). To classify jobs in sectors, I follow the classification by the French National Institute of Statistics and Economic Studies of four sectors: agriculture, manufacturing, public, and service. For each municipality and time period, I compute and use as outcome the share of a given sector in the local labor force (in percent).

Table 4 shows that agricultural mechanization have indeed led to a reduction in the share of agricultural jobs to the benefit of the share of manufacturing jobs. A 0.8 percentage point decline in the share of agricultural workers is compensated by a 1.1 percentage point increase in the share of manufacturing workers. This finding is evidence of local structural transformation following the increased mechanization of agricultural production, and directly in line with macroeconomic studies (Herrendorf, Rogerson, and Valentinyi, 2014, review the literature). The shares of jobs in the service and public sectors appear mostly unaffected by the reforms. No significant pre-trends are observed in the considered outcomes.

Table 4: Mechanization and economic transformation

	(1)	(2)	(3)	(4)
	Employment share in:			
	agriculture	manufacturing	services	public sector
Unit:	(%)	(%)	(%)	(%)
Treatment effect	-0.771***	1.069***	-0.240	-0.057
	(0.295)	(0.244)	(0.262)	(0.154)
Pre-trend $t-1$	0.948	0.071	-0.862	-0.157
	(0.648)	(0.527)	(0.555)	(0.334)
Pre-trend $t-2$	-0.467	0.119	0.413	-0.064
	(0.627)	(0.518)	(0.558)	(0.322)
Obs.	63399	63399	63399	63399
Mean dep. var.	26.844	20.441	43.232	9.481

Notes: Table reports the estimated effect of land consolidation on municipal sectoral labor shares using a difference-in-differences design with staggered treatment adoption following Borusyak et al. (2021). Municipal labor shares (at the workplace) are observed between 1968 and 2015.

5.4 Female labor force participation

Using difference-in-differences, Table 5 investigates the consequences of mechanization for female labor force participation. Two main results appear. First, the overall female labor share increased by 0.3 percentage point for the average municipality. Second, the increase was not smooth across sectors. The share of female working in agriculture and manufacturing declined, whereas more women went to work for the service and public sectors. A 0.6 percentage point and a 0.1 percentage point increase in the female labor share in the public and service sectors are observed, respectively.

Table 5: Mechanization and female labor force participation

	(1)	(2)	(3)	(4)	(5)
	Overall female	Female employment share in:			
	employment share	agriculture	manufacturing	services	public sector
Unit:	(%)	(%)	(%)	(%)	(%)
Treatment effect	0.294***	-0.221***	-0.176***	0.580***	0.112***
	(0.079)	(0.051)	(0.029)	(0.058)	(0.007)
Pre-trend $t-1$	0.366**	0.436***	0.010	-0.088	0.008
	(0.169)	(0.132)	(0.065)	(0.109)	(0.018)
Pre-trend $t-2$	-0.162	-0.148	-0.002	-0.007	-0.005
	(0.168)	(0.118)	(0.067)	(0.116)	(0.018)
Obs.	63406	63406	63406	63406	63406
Mean dep. var.	8.988	1.977	1.469	5.410	0.130

Notes: Table reports the estimated effect of land consolidation on municipal female labor market participation using estimating a difference-in-differences design with staggered treatment adoption following Borusyak et al. (2021). Female labor participation is further divided by economic sectors. Municipal labor shares (at the workplace) are observed between 1968 and 2015.

6 Effect on voting behavior

Following findings on the impact of automation on voting bahavior (Frey et al., 2018; Bó et al., 2018; Im et al., 2019; Dijkstra et al., 2020; Guriev and Papaioannou, 2020; Anelli et al., 2021), I start by studying the impact of mechanization on the far-right vote share, before turning to the vote share of other parties. Finally, I present a series of robustness tests.

6.1 Results on far-right vote shares

Spatial RDD results. Table 6 reports the estimation of the RD approach on the far-right vote share. The outcome is the average far-right vote share around the border across the first rounds of the 2002, 2007, 2012 and 2017 French presidential elections. Outcome is measured at the municipal level. Far-right vote share refers to the vote share for the *Front National* – the leading far-right party with wide coverage across the country – plus smaller nationalist parties. Alternatively, I present a robustness test using only the *Front National* vote share as the far-right below. Results are qualitatively and qualitatively very similar. Panel (a) reports results using a regression discontinuity approach, whereas Panel (b) reports results using a fuzzy regression discontinuity approach where distance to the soil composition border is used as running variable in a first stage. First stage results are also reported. Columns (1), (2) and (3) use the optimal bandwidth following Calonico et al. (2014) without regional effects, with regional fixed effects, and with regional fixed effects and covariates, respectively.

Table 6: MECHANIZATION AND THE AVERAGE FAR-RIGHT VOTE SHARE

	(1)	(2)	(3)
		(a) Sharp RD design	
Treatment effect (%p)	1.460***	1.122***	1.198***
	(0.382)	(0.363)	(0.356)
Obs.	4,887	4,887	4,887
Bandwidth (km)	18.2	18.2	18.2
Obs. bw.	1,734	1,734	1,734
		(b) Fuzzy RD design	
Treatment effect (%p)	1.050***	0.901***	0.903***
	(0.231)	(0.274)	(0.267)
Dist. soil border (1st stage)	1.280***	1.071***	1.071***
	(0.098)	(0.083)	(0.082)
Obs.	4,887	4,887	4,887
Bandwidth (km)	30.4	30.4	30.4
Obs. bw.	2,428	2,428	2,428
Department FE	No	Yes	Yes
Covariates	No	No	Yes
Bandwidth	Opt	Opt	Opt
Mean dep. var.		19.757	

Notes: Table reports local polynomial regression-discontinuity estimation with robust bias-corrected confidence intervals and inference procedures following Calonico et al. (2014). The outcome is the average far-right vote share around the border across the first rounds of the 2002, 2007, 2012 and 2017 French presidential elections. Formal robustness test to bandwidth choice is presented in Figure A13. Mean of dependent variable is computed using the optimal bandwidth.

A significant positive effect is observed above the threshold across specifications. The average far-right vote share is about 1.2 percentage point – or 6.1% relative to the average far-right vote share – higher in the area that engaged more in mechanisation and land consolidation. This is in line with the general finding in the automation and populism literature cited above.

Regression discontinuity (RD) plots. Figure 7 shows how land consolidation reform border affects the share of far-right vote (in percent) using a data-driven regression-discontinuity plot following Calonico et al. (2014). In line with results in Table 6, an highly significant positive jump – of about 2 percentage points – at the border is observed. Mechanization induced by land consolidation appears to have lead to a long-term increase in the share of far-right votes.

Figure 7: FAR-RIGHT VOTING SHARES AROUND THE CUTOFF (MUNICIPAL LEVEL, 2002-2017)

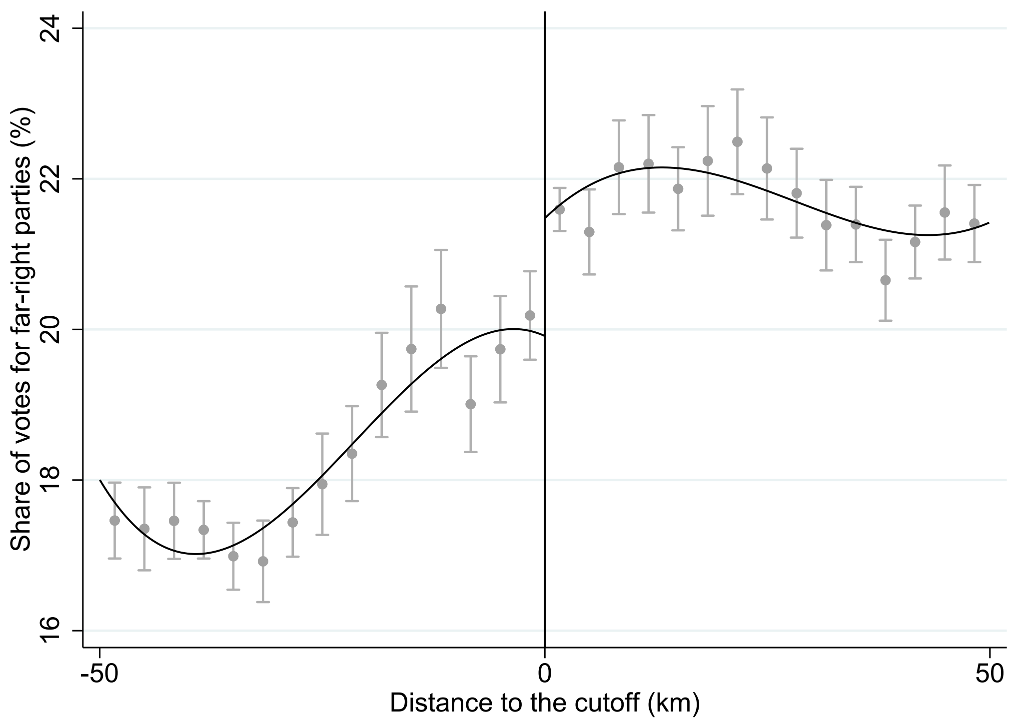

Notes: Data-driven regression-discontinuity plots following Calonico et al. (2014). 95% confidence intervals are presented. Share of far-right vote is the average share of far-right vote across the first rounds of the presidential elections in 2002, 2007, 2012 and 2017 at the municipal level.

I conduct a series of robustness tests to further assess the validity of the results on the far-right vote share. I proceed in three steps. First, I exploit *Seuil du Poitou* to insure that mechanization – and not regional fundamentals – explain the effect observed. Second, I present placebo tests to investigate how the treatment effect evolves when "shifting" East-/Westward the threshold. Finally, I study how the treatment effect varies with the definition of the "far-right".

Robustness using the *Seuil du Poitou*. As for population and employment, I use the sub-sample of municipalities located on the *Seuil du Poitou* to insure that the observed voting behavior patterns are not related to regional characteristics (e.g., distance to the Paris basin). Formally, I replicate the approach in 6 on this sub-sample. The results are presented in Table A8. In line with the hypothesis that a discontinuity in land consolidation – and subsequent mechanization – led to a gap in the far-right vote share, the absence of such discontinuity is associated with the absence of a gap in the far-right vote share.

Robustness using placebo border shifts. I investigate how the treatment effect varies when shifting the threshold East-/Westward. Formally, I shift the threshold by ±5km, ±7km, ±15km and ±30km. Table A11 reports the results. The actual threshold is labeled: *baseline*. As in Table 6, the dependent variable is the average share of far-right vote across the 2002, 2007, 2012 and 2017 French presidential elections. A significant effect is observed *only* for the actual border. The magnitude of the estimated coefficient is also closer to 0 for all placebo borders.

Robustness using alternative bandwidth sizes. In this paper, whenever estimating a RD design, I employed the optimal bandwidth selection criteria proposed by Calonico et al. (2014). Despite the clear advantages of using such bandwidth, it appears useful to investigate how sensitive are the results to the bandwidth size. Figure A13 presents a series of local polynomial regression-discontinuity estimation where the bandwidth size varies from 0.5 times the optimal bandwidth to 2 times the optimal bandwidth, with 0.25 increments. Following Calonico et al. (2014), the optimal bandwidth is 18.173km. Overall, the bandwidth size appears to have little effect on the results, both in terms of point estimated and confidence intervals.

Robustness using an alternative definition of the far-right: *Front National* vote share only. In Table 6, the far-right segment of the political spectrum is defined as the sum of parties traditionally considered far-right. These include the *Front National* (i.e., most popular far-right party), but also a set of smaller nationalist parties such as the *National Republican Movement*. As smaller nationalist parties may have heterogeneous local ties, I study the far-right vote share defined solely as the *Front National* in Table A12. Results are qualitatively and quantitatively very similar.

6.2 Are other parties and turnout also affected?

Table A13 estimates the effect of mechanization on turnout and on the voting share of non-far right party groups. As comparison, the estimation approach in Table A13 is analogous to column 3 in Table 6. Turnout appears mostly unaffected, whereas the vote share of the extreme left and the center right declines on the border side of the Paris basin. This supports the *horseshoe hypothesis* according to which the voting space is closer to a circle than a line such that the extreme may "touch". The far-right gain came from "spatially" close parties. This is not to say that the programs of the far-right and far-left are similar, but instead that the far-right is able to source voters from the far-left (even if center left parties are unaffected). To complete this analysis, Figure A9 provides RD plots focusing alternatively on voter turnout (Panel a), and on all other party groups (Panels b-d).

6.3 Far-right vote share over time

French municipal voting data are only available back in time (from 1965 onwards) *at the department level* (NUTS3). This prevents the estimation of a difference-in-differences design where the treatment status is a dummy defined at the municipal level. Yet, the share of consolidated municipalities within a department at the time of the different French presidential elections since 1965 can be used to capture how land consolidation and mechanization have affected the far-right vote share over time.

Figure A14 shows visually the correlation between the share of consolidated municipalities and the far-right vote share using department-presidential-election-year observations between 1965 and 2017. A clear positive relationships appears. This result is confirmed using a two-way fixed effects approach in Table A14. Columns (1), (2) and (3) shows the result of linearly regressing the departmental far-right vote share on the departmental share of consolidated municipalities without, with year, and with year and department fixed effects, respectively. A 1% increase in the share of consolidated municipalities is associated with a 0.1 percentage point increase in the far-right vote share.

7 Mechanism

The results from Sections 5 and 6 are puzzling as a rise in populism is often associated to an economic downturn. For instance, the literature highlights the role of economic decline as well as the importance of economic and financial crises in explaining observed increases in populism (see, e.g., de Bromhead, Eichengreen, and O'Rourke, 2012; Funke, Schularick, and Trebesch, 2016; Algan, Guriev, Papaioannou, and Passari, 2017; Dijkstra et al., 2020; Guriev and Papaioannou, 2020; Doerr, Gissler, Peydró, and Voth, 2022). Yet, in this paper, mechanization appears to lead to both economic growth and a rise in support for the far-right.

Whereas this finding may *a priori* be surprising, the political economy literature calls attention to determinants of populism independent of economic decline: immigration, as well as non-monetary outcomes related to local identities can cause far-right sentiments to rise. In what follows, we study both mechanisms successively.

7.1 The role of immigration

Immigration has long been recognized as a driver of populist vote, independently of actual economic outcomes (Barone et al., 2016; Halla et al., 2017; Becker et al., 2017; Dustmann et al., 2018). In Table 7, I test for possible effects of consolidation and subsequent mechanization on migration. In columns (1) and (2), I report the results of estimating a difference-in-differences design following Borusyak et al. (2021) on natural demographic gain (per 100 residents) and net migration (per 100 residents), respectively. Both outcomes are observed between 1968 and 2015. Municipalities on the mechanization side of the border appear to host 3.1 more migrants per 100 residents after consolidation, with a small effect already observable at $t-1$. Natural demographic growth – defined as the difference between births and deaths between two census waves – appears unaffected.

To capture the location of origin of the positive effect on net migration, I focus on the long term density of residents by birthplace in columns (3), (4) and (5). I use data from the 2015 population census at the municipal level. Birthplace is categories in three groups: (i) in the same department (NUTS3 of the EU regional categorization) as the municipality, (ii) in the rest of France, including overseas territories, (iii) out of France. To capture the growth effect of each group independently of the municipal population growth observed in Table 2, I normalize each outcome by the municipal area (and not by population). I find that municipalities on the Paris basin side of the mechanization border have a higher share of foreign born residents and of France-born residents with birthplace outside of the department. The density of residents born in the same department does not differ around the mechanization border. I interpret this result as evidence that land consolidation reforms – and the subsequent mechanization – led to the arrival of migrants from out of the department with a significant share from abroad.

Table 7: Population growth from natural growth or in-migration?

	(1)	(2)	(3)	(4)	(5)
	DiD		Spatial RDD		
	Natural	Net	Resident with birthplace in:		
	demographic growth	migration	same region	rest of France	abroad
Unit:	(per 100 residents)	(per 100 residents)	(per ha)	(per ha)	(per ha)
Treatment effect	-0.120	3.076***	0.091	0.103**	0.036***
	(0.098)	(0.313)	(0.061)	(0.040)	(0.012)
Pre-trend $t-1$	0.047	1.096*	-	-	-
	(0.161)	(0.608)			
Pre-trend $t-2$	-0.041	-0.640	-	-	-
	(0.167)	(0.600)			
Bandwidth (km)	-	-	19.2	26.8	26.1
Obs. bw.	-	-	1,786	2,223	2,191
Obs.	55,464	55,464	4,888	4,888	4,888
Mean dep. var.	0.869	4.488	0.395	0.306	0.047

Notes: In columns 1 and 2, I report the results of estimating a difference-in-differences design with staggered treatment adoption following Borusyak et al. (2021). Natural growth and net migration are observed between 1968 and 2015. In columns 3-5, I focus on the long term density of residents by birthplace. Data from 2015 is then used. Birthplace is categories in three groups: (i) in the same department (NUTS3 region in EU regional categorization) as the municipality, (ii) in the rest of France, including overseas territories, (iii) out of France.

7.2 The role of local identity

The observed effect on the far-right vote share may also be related to nonmonetary ouctomes. For instance, recent work has highlighted the role of identity (Fukuyama, 2018; Noury and Roland, 2020; Mutz, 2018) in the rise in populism observed in many countries of the Western World. Geographers have also spotlighted the impact of mechanization on important transformation of rural identities (Bailoni, 2012).

The effects of mechanization on the local economic organization and female labor force participation – presented in Sections 5.3 and 5.4 – constitute a first set of evidence that mechanization induces large societal changes in the rural world. Voters may view negatively the transformation of their localities as less workers work directly in agriculture, and as farms are getting increasingly mechanised. A feeling of not "recognizing" their municipality may prompt a reaction towards reactionary sentiments.

To further test for this mechanism, the historical French agricultural censuses record information on the composition of farms. Traditionally, the family farm model – where both spouses, and possibly other family members, work on the farm – has dominated. As mechanization took off, the need for other family members besides the head of the farm decreased; thus, changing the farm model from family to a more professional organization.

Using the agricultural census since 1970 in a DiD approach, Table 8 studies how mechanization has impacted the absolute number (columns 1-3) and the labor share (columns 4-6) of farm heads, spouses, and other family members working on the farm. I observe that increased mechanization led to the decline in the absolute number of spouses working on the farms. For the average municipality, I estimated that 2.6 spouses stopped working on family farms. Even though the data does not specify whether the spouse was male or female, the traditional family organization makes it very likely that female spouses were mostly affected. Mechanically, this led to an increase in the labor share of farm head and a decline in the share of spouses. The number and share of other family members working on the farm appears unaffected by the reforms. Note that a small (barely significant) decline in the number and share of spouses working on the farm is observed already one period before treatment (i.e., between 1 and 7 years before).

Table 8: Worker structure of agricultural firms

	(1)	(2)	(3)	(4)	(5)	(6)
	Absolute count			Share of municipal agricultural workers		
	Farm head	Spouse	Other family	Farm head	Spouse	Other family
Unit:	(Count)	(Count)	(Count)	(%)	(%)	(%)
Treatment effect	0.280	-2.684***	-0.188	1.770***	-2.011***	-0.154
	(0.352)	(0.326)	(0.333)	(0.126)	(0.126)	(0.153)
Pre-trend $t-1$	0.606	-1.393**	-0.660	0.428	-0.917*	-0.413
	(0.686)	(0.707)	(0.839)	(0.363)	(0.477)	(0.546)
Pre-trend $t-2$	0.962	0.465	0.645	0.503	0.616	-0.425
	(0.635)	(0.591)	(0.674)	(0.366)	(0.454)	(0.534)
Obs.	164,282	164,282	164,282	150,469	150,469	150,469
Mean dep. var.	32.335	16.477	9.533	51.201	19.248	9.761

Notes: Table reports the results of estimating a difference-in-differences design with staggered treatment adoption following Borusyak et al. (2021). It studies how mechanization has impacted the absolute number (columns 1-3) and the labor share (columns 4-6) of farm heads, spouses, and other family members working on the farm. Data from the historical agricultural censuses since 1970 are used.

8 Conclusion

This paper investigates the causal economic and political effects of agricultural mechanization. It exploits a spatial discontinuity in the intensity of mechanization – induced by variation in the intensity of land consolidation reforms in France since 1945 – in a Spatial Regression Discontinuity Design.

Studying both economic and political outcomes in the long-run, I find that mechanization leads to a long-term growth in population, employment and income, but also to an increase in far-right voting. Guided by the political economy literature, I show that two main societal changes caused by mechanization may explain the rise in populism despite the good economic situation. First, mechanization appears to have induced larger immigration flows to treated municipalities; and especially, of migrants born outside of France. Second, mechanization also appears to have had large effects on the local socio-economic organization, with labor shifts away from agriculture, and a decline in the traditional family-ran farm model in favor of more mechanized and professional structures.

The results presented in this paper have a key consequence for future policy design. This paper shows that mechanization is causing a rise of the far-right vote share, *despite local economic gains*. Hence, the rise in populism in agricultural areas is unlikely to be mitigated by place-based policies centered around improving the local economic situation. Instead, accounting for the local socio-economic concerns is more likely to deliver positive results.

References

Daron Acemoglu and David Autor. Skills, Tasks and Technologies: Implications for Employment and Earnings. In O. Ashenfelter and D. Card, editors, *Handbook of Labor Economics*, volume 4 of *Handbook of Labor Economics*, chapter 12, pages 1043–1171. Elsevier, 2011. URL https://ideas.repec.org/h/eee/labchp/5-12.html.

Daron Acemoglu and Pascual Restrepo. The race between man and machine: Implications of technology for growth, factor shares, and employment. *American Economic Review*, 108(6):1488–1542, June 2018. doi: 10.1257/aer.20160696. URL https://www.aeaweb.org/articles?id=10.1257/aer.20160696.

Daron Acemoglu and Pascual Restrepo. Automation and new tasks: How technology displaces and reinstates labor. *Journal of Economic Perspectives*, 33(2):3–30, May 2019. doi: 10.1257/jep.33.2.3. URL https://www.aeaweb.org/articles?id=10.1257/jep.33.2.3.

Daron Acemoglu and Pascual Restrepo. Tasks, Automation, and the Rise in US Wage Inequality. NBER Working Papers 28920, National Bureau of Economic Research, Inc, June 2021. URL https://ideas.repec.org/p/nbr/nberwo/28920.html.

Tjitske Akkerman. Gender and the radical right in western europe: a comparative analysis of policy agendas. *Patterns of Prejudice*, 49(1-2):37–60, 2015.

Yann Algan, Sergei Guriev, Elias Papaioannou, and Evgenia Passari. The european trust crisis and the rise of populism. *Brookings Papers on Economic Activity*, pages 309–382, 2017. ISSN 00072303, 15334465. URL http://www.jstor.org/stable/90019460.

Ethem Alpaydin. *Introduction to machine learning*. MIT press, 2020.

Massimo Anelli, Italo Colantone, and Piero Stanig. Individual vulnerability to industrial robot adoption increases support for the radical right. *Proceedings of the National Academy of Sciences*, 118(47):e2111611118, 2021.

David H. Autor and David Dorn. The growth of low-skill service jobs and the polarization of the us labor market. *American Economic Review*, 103(5):1553–97, August 2013. doi: 10.1257/aer.103.5.1553. URL https://www.aeaweb.org/articles?id=10.1257/aer.103.5.1553.

Mark Bailoni. Identités, territoires et paysages ruraux en mutations. *Revue Géographique de l'Est*, 52(3-4), 2012.

Guglielmo Barone, Alessio D'Ignazio, Guido de Blasio, and Paolo Naticchioni. Mr. rossi, mr. hu and politics. the role of immigration in shaping natives' voting behavior. *Journal of Public Economics*, 136:1–13, 2016. ISSN 0047-2727. doi: https://doi.org/10.1016/j.jpubeco.2016.03.002. URL https://www.sciencedirect.com/science/article/pii/S0047272716000414.

Sascha O Becker, Thiemo Fetzer, and Dennis Novy. Who voted for Brexit? A comprehensive district-level analysis. *Economic Policy*, 32(92):601–650, 10 2017. ISSN 0266-4658. doi: 10.1093/epolic/eix012. URL https://doi.org/10.1093/epolic/eix012.

Ernesto Dal Bó, Frederico Shimizu Finan, Olle Folke, Torsten Persson, and Johanna Rickne. Economic losers and political winners: Swedenâ€™s radical right. 2018.

Kirill Borusyak, Xavier Jaravel, and Jann Spiess. Revisiting Event Study Designs: Robust and Efficient Estimation. Papers 2108.12419, arXiv.org, August 2021.

Sebastian Calonico, Matias D. Cattaneo, and Rocio Titiunik. Robust nonparametric confidence intervals for regression-discontinuity designs. *Econometrica*, 82(6):2295–2326, 2014.

Sebastian Calonico, Matias D. Cattaneo, Max H. Farrell, and RocÃo Titiunik. Regression Discontinuity Designs Using Covariates. *The Review of Economics and Statistics*, 101(3):442–451, July 2019.

Sebastian Calonico, Matias Cattaneo, and Max Farrell. Optimal bandwidth choice for robust bias corrected inference in regression discontinuity designs. *The Econometrics Journal*, 23, 11 2020. doi: 10.1093/ectj/utz022.

Julieta Caunedo and Namrata Kala. Mechanizing agriculture. Working Paper 29061, National Bureau of Economic Research, July 2021. URL http://www.nber.org/papers/w29061.

Wolfgang Dauth, Sebastian Findeisen, Jens Suedekum, and Nicole Woessner. Adjusting to Robots: Worker-Level Evidence. Opportunity and Inclusive Growth Institute Working Papers 13, Federal Reserve Bank of Minneapolis, August 2018. URL https://ideas.repec.org/p/fip/fedmoi/0013.html.

Alan de Bromhead, Barry Eichengreen, and Kevin O'Rourke. Right-wing political extremism in the great depression. NBER Working Papers 17871, National Bureau of Economic Research, Inc, 2012. URL https://EconPapers.repec.org/RePEc:nbr:nberwo:17871.

Klaus Deininger, Songqing Jin, and Fang Xia. *Moving off the Farm: Land Institutions to Facilitate Structural Transformation and Agricultural Productivity Growth in China*. The World Bank, 2012. doi: 10.1596/1813-9450-5949. URL https://elibrary.worldbank.org/doi/abs/10.1596/1813-9450-5949.

Klaus Deininger, Daniel Monchuk, Hari K Nagarajan, and Sudhir K Singh. Does land fragmentation increase the cost of cultivation ? evidence from India. Policy Research Working Paper

Series 7085, The World Bank, November 2014. URL https://ideas.repec.org/p/wbk/wbrwps/7085.html.

Lewis Dijkstra, Hugo Poelman, and AndrÃ©s Rodríguez-Pose. The geography of eu discontent. *Regional Studies*, 54(6):737–753, 2020. URL https://EconPapers.repec.org/RePEc:taf:regstd:v:54:y:2020:i:6:p:737-753.

Sebastian Doerr, Stefan Gissler, José-Luis Peydró, and Hans-Joachim Voth. Financial crises and political radicalization: How failing banks paved hitler's path to power. *The Journal of Finance*, n/a(n/a), 2022. doi: https://doi.org/10.1111/jofi.13166. URL https://onlinelibrary.wiley.com/doi/abs/10.1111/jofi.13166.

Christian Dustmann, Kristine Vasiljeva, and Anna Piil Damm. Refugee Migration and Electoral Outcomes. *The Review of Economic Studies*, 86(5):2035–2091, 09 2018. ISSN 0034-6527. doi: 10.1093/restud/rdy047. URL https://doi.org/10.1093/restud/rdy047.

Carl Benedikt Frey, Thor Berger, and Chinchih Chen. Political machinery: did robots swing the 2016 US presidential election? *Oxford Review of Economic Policy*, 34(3):418–442, 07 2018. ISSN 0266-903X. doi: 10.1093/oxrep/gry007. URL https://doi.org/10.1093/oxrep/gry007.

Francis Fukuyama. Identity: The demand for dignity and the political of resentment. 2018.

Manuel Funke, Moritz Schularick, and Christoph Trebesch. Going to extremes: Politics after financial crises, 1870â€"2014. *European Economic Review*, 88(C):227–260, 2016. URL https://EconPapers.repec.org/RePEc:eee:eecrev:v:88:y:2016:i:c:p:227-260.

Claudia Goldin and Lawrence F. Katz. The origins of technology-skill complementarity. *The Quarterly Journal of Economics*, 113(3):693–732, 1998. ISSN 00335533, 15314650. URL http://www.jstor.org/stable/2586871.

Maarten Goos, Alan Manning, and Anna Salomons. Explaining job polarization: Routine-biased technological change and offshoring. *American Economic Review*, 104(8):2509–26, August 2014. doi: 10.1257/aer.104.8.2509. URL https://www.aeaweb.org/articles?id=10.1257/aer.104.8.2509.

Georg Graetz and Guy Michaels. Robots at Work. *The Review of Economics and Statistics*, 100(5):753–768, 12 2018. ISSN 0034-6535. doi: 10.1162/rest_a_00754. URL https://doi.org/10.1162/rest_a_00754.

Sergei Guriev and Elias Papaioannou. The political economy of populism. CEPR Discussion Papers 14433, C.E.P.R. Discussion Papers, 2020. URL https://EconPapers.repec.org/RePEc:cpr:ceprdp:14433.

Jinyong Hahn, Petra Todd, and Wilbert Van der Klaauw. Identification and Estimation of Treatment Effects with a Regression-Discontinuity Design. *Econometrica*, 69(1):201–209, January 2001. URL https://ideas.repec.org/a/ecm/emetrp/v69y2001i1p201-09.html.

Martin Halla, Alexander F. Wagner, and Josef Zweimüller. Immigration and voting for the far right. *Journal of the European Economic Association*, 15(6):1341–1385, 2017. URL https://EconPapers.repec.org/RePEc:oup:jeurec:v:15:y:2017:i:6:p:1341-1385.

John A Hartigan and Manchek A Wong. Algorithm as 136: A k-means clustering algorithm. *Journal of the royal statistical society. series c (applied statistics)*, 28(1):100–108, 1979.

Leander Heldring, James A Robinson, and Sebastian Vollmer. The economic effects of the english parliamentary enclosures. Working Paper 29772, National Bureau of Economic Research, February 2022. URL http://www.nber.org/papers/w29772.

Berthold Herrendorf, Richard Rogerson, and Akos Valentinyi. Chapter 6 - growth and structural transformation. In Philippe Aghion and Steven N. Durlauf, editors, *Handbook of Economic Growth*, volume 2 of *Handbook of Economic Growth*, pages 855–941. Elsevier, 2014. doi: https://doi.org/10.1016/B978-0-444-53540-5.00006-9. URL https://www.sciencedirect.com/science/article/pii/B9780444535405000069.

Zhen Im, Nonna Mayer, Bruno Palier, and Jan Rovny. The "losers of automation": A reservoir of votes for the radical right? *Research Politics*, 6:205316801882239, 03 2019. doi: 10.1177/2053168018822395.

James M. MacDonald. Tracking the consolidation of u.s. agriculture. *Applied Economic Perspectives and Policy*, 42(3):361–379, 2020. doi: https://doi.org/10.1002/aepp.13056. URL https://onlinelibrary.wiley.com/doi/abs/10.1002/aepp.13056.

James M. MacDonald, Robert A. Hoppe, and Doris Newton. Three decades of consolidation in u.s. agriculture. (1476-2018-5467), 2018. doi: 10.22004/ag.econ.276247. URL http://ageconsearch.umn.edu/record/276247.

K. Marx. *Das Kapital*. London, Penguin., 1990.

Michael McCormick, Guoping Huang, Giovanni Zambotti, and Jessica Lavash. Roman Road Network (version 2008), 2013.

Diana C. Mutz. Status threat, not economic hardship, explains the 2016 presidential vote. *Proceedings of the National Academy of Sciences*, 115(19):E4330–E4339, 2018. doi: 10.1073/pnas.1718155115. URL https://www.pnas.org/doi/abs/10.1073/pnas.1718155115.

Abdul Noury and Gerard Roland. Identity politics and populism in europe. *Annual Review of Political Science*, 23(1):421–439, 2020.

Julien Perret, Maurizio Gribaudi, Marc Barthelemy, Nathalie Abadie, Stéphane Baciocchi, Carlo Bertelli, Olivier Bonin, Patricia Bordin, Benoît Costes, Pascal Cristofoli, Bertrand Dumenieu, Julie Gravier, Jean-Paul Hubert, Pierre-André Le Ny, Eric Mermet, Claude Motte, Mylène Pardoen, Ana-Maria Raimond, Sandrine Robert, and Marie-Christine Vouloir. The 18th century Cassini roads and cities dataset, 2015.

Marc-André Philippe and Nadine Polombo. Soixante années de remembrement : essai de bilan critique de l'aménagement foncier en France. In *70 ans d'aménagement foncier en France : Principes, méthodes et évolution, comparaison avec d'autres expériences en Europe et dans le monde*, pages 33–41, Lyon, France, September 2013.

Prabhu Pingali. Chapter 54 agricultural mechanization: Adoption patterns and economic impact. In R. Evenson and P. Pingali, editors, *Agricultural Development: Farmers, Farm Production and Farm Markets*, volume 3 of *Handbook of Agricultural Economics*, pages 2779–2805. Elsevier, 2007. doi: https://doi.org/10.1016/S1574-0072(06)03054-4. URL https://www.sciencedirect.com/science/article/pii/S1574007206030544.

Paul A. Samuelson. The pure theory of public expenditure. *The Review of Economics and Statistics*, 36(4):387–389, 1954. ISSN 00346535, 15309142. URL http://www.jstor.org/stable/1925895.

Niels Spierings and Andrej Zaslove. Gendering the vote for populist radical-right parties. *Patterns of Prejudice*, 49(1-2):135–162, 2015.

United States. Bureau of the Census and United States. Bureau of Agricultural Economics. *United States Census of Agriculture: 1950*. Number v. 1, pt. 29 in United States Census of Agriculture: 1950. U.S. Government Printing Office, 1952. URL https://books.google.ch/books?id=IhjolY0GCs8C.

Arvo Vitikainen. An overview of land consolidation in europe. *Nordic Journal of Surveying and Real Estate Research*, 1(1), Apr. 2014. URL https://journal.fi/njs/article/view/41504.

Appendix for
"Land Consolidation Reforms: A Natural Experiment on the Economic and Political Effects of Agricultural Mechanization"
(for online publication only)

G. Loumeau

A Supporting Material

A.1 Tables

Table A1: DESCRIPTIVE STATISTICS: MUNICIPAL LEVEL

	N	Average value	Standard deviation
	(a) Population		
Population (1876)	34401	1050.749	4032.016
Population (1901)	34401	1094.251	5481.072
Population (1936)	34401	1125.977	7760.287
Population (1968)	34401	1362.904	8822.474
Population (1990)	34401	1573.526	8532.082
Population (2015)	34401	1792.824	9410.432
	(b) Labor		
Workers (1968)	34401	322.443	2180.553
...in agriculture (1968)	34401	47.678	62.271
...in manufacturing (1968)	34401	95.547	639.115
...in services (1968)	34401	143.986	1345.986
...in public (1968)	34401	35.232	230.673
Female workers (1968)	34401	97.733	726.054
Workers (1990)	34401	475.561	2515.583
...in agriculture (1990)	34401	23.600	33.543
...in manufacturing (1990)	34401	112.500	465.684
...in services (1990)	34401	304.293	1915.65
...in public (1990)	34401	35.166	163.330
Female workers (1990)	34401	198.172	1117.202
Workers (2015)	34401	520.228	3821.053
...in agriculture (2015)	34401	13.335	26.16278
...in manufacturing (2015)	34401	70.445	366.3425
...in services (2015)	34401	400.906	3325.938
...in public (2015)	34401	35.540	195.0574
Female workers (2015)	34401	252.140	1924.1

Notes: Table continues on the next page.

TABLE A1: DESCRIPTIVE STATISTICS: MUNICIPAL LEVEL (*CONTINUED*)

	N	**Average value**	**Standard deviation**
	(c) Land consolidation		
Year consolidation	16303	1972.888	15.079
Area consolidated (ha)	16303	848.247	742.716
	(d) Voting		
Average turnout	34401	80.996	3.786
Average far-right vote share	34386	21.812	5.321
Average right vote share	34386	44.765	6.661
Average left vote share	34386	23.468	6.196
Average far-left vote share	34386	9.953	2.444
	(e) Income		
Average median income (€/year)	26443	18304.82	2899.195

Notes: Population and labor information are taken from the French official censuses. Land consolidation information is extracted from the land consolidation database by Philippe and Polombo (2013). Electoral averages are taken over the first rounds of the presidential elections in 2002, 2007, 2012 and 2017. Municipal median income is only available in municipalities with at least 50 households for confidentiality reasons.

Table A2: Descriptive statistics: 200m2 cell level

	N	Average value	Standard deviation
	(a) Population		
N. individuals	468632	16.024	36.404
N. households	468632	7.035	17.844
	(b) Income		
Income pc (€/year)	468632	21458.63	3031.752
Total income (€/year)	468632	340516	721155.5
Fr. poor households	468632	.120	.098

Notes: Gridded data at 200m2 from 2015. To respect individual data confidentiality, individual incomes are winsorized the 5th and 95th percentiles of the departmental (NUTS3) individual income distribution.

Table A3: Historical and fundamental balancing tests

	(1)	(2)	(3)	(4)	(5)
	Historical population				
	(a) *1876*	(b) *1881*	(c) *1886*	(d) *1891*	(e) *1896*
Treatment	115.468	145.487	160.616	161.196	174.035
	(153.011)	(164.458)	(171.009)	(170.958)	(174.313)
Bandwidth (km)	31.1	30.9	30.8	30.6	30.9
Obs. bw.	2,389	2,376	2,369	2,361	2,375
Mean dep var	1,234	1,245	1,258	1,246	1,224
	Historical population				
	(f) *1901*	(g) *1906*	(h) *1911*	(i) *1921*	(j) *1926*
Treatment	198.175	215.206	227.461	246.866	269.213
	(179.910)	(181.241)	(183.845)	(181.636)	(182.593)
Bandwidth (km)	30.8	30.6	30.7	31.5	31.4
Obs. bw.	2,368	2,358	2,362	2,404	2,403
Mean dep var	1,218	1,186	1,203	1,104	1,101
	Historical population		**Municipal fundamental**		
	(k) *1931*	(l) *1936*	(m) *Area*	(n) *River*	(o) Avg. elevation
Treatment	289.759	313.165	146.113	-0.014	6.587
	(185.720)	(194.030)	(180.353)	(0.030)	(5.874)
Bandwidth (km)	31.2	31.5	19.6	23.9	19.1
Obs. bw.	2,393	2,404	1,817	1,997	1,784
Mean dep var	1,091	1,091	2,220	.106	136

Notes: Table continues on the next page.

Table A4: Historical and fundamental balancing tests (*continued*)

	(1)	(2)	(3)	(4)	(5)
	Mun. Fund.	**Trans. net.**		**Urbanization**	
	(p) *Std. elevation*	(q) *Roman road*	(r) *Cassini road*	(s) *Cassini settlement*	(t) *Area Cassini settlement*
Treatment	0.070	-0.017	-0.017	0.028	0.057
	(0.691)	(0.039)	(0.039)	(0.119)	(0.073)
Bandwidth (km)	19.7	27.7	27.7	47.3	22.4
Obs. bw.	1,817	2,203	2,203	481	296
Mean dep var	14.9	.275	.275	1.19	.152

Notes: Table reports local polynomial regression-discontinuity estimation with robust bias-corrected confidence intervals and inference procedures following Calonico et al. (2014). Area refers to the municipal area and is measured in km2. Area of Cassini settlement is measured in m/km2. River, roman road, Cassini road, Cassini settlement refers to the presence of a river, a roman road, a Cassini road and a Cassini settlement in the municipality, respectively. Elevation measures are based on the EU's 2018 layer of the Copernicus Land Monitoring Service (spatial resolution of 25m). Geo-localized information on the placement of roman roads circa 117 AD is derived from (Harvard Dataverse, McCormick, Huang, Zambotti, and Lavash, 2013). Geo-localized information on the historical placement of roads is obtained from the 18th century Cassini roads dataset (Harvard Dataverse, Perret et al., 2015).

Table A5: DIFFERENCE-IN-DIFFERENCES: MECHANIZATION, POPULATION AND EMPLOYMENT

	(1) Municipal population	(2) Municipal employment	(3) Employment to population
Treatment effect	161.053***	21.297***	1.292***
	(54.176)	(5.041)	(0.140)
Pre-trend $t-1$	-76.816***	-10.327*	0.475
	(17.805)	(6.027)	(0.303)
Pre-trend $t-2$	-34.092	-7.541	-0.187
	(22.825)	(6.870)	(0.277)
Obs.	437,427	64,232	63,406
Mean dep. var.	982.509	272.067	24.212

Notes: Table reports the estimated effect of land consolidation on municipal residential (column 1) and job (column 2) count, respectively. Column (3) focuses on the number of workers *at the workplace* per capita within the municipality. I report the results of estimating a difference-in-differences design with staggered treatment adoption following Borusyak et al. (2021). Municipal population count is observed between 1876 and 2015, whereas municipal job count is observed between 1968 and 2015.

Table A6: Results on population:
Robustness using municipalities on the *Seuil du Poitou*

	(1)	(2)	(3)	(4)	(5)	(6)
	Population count		Population density		Population growth (%p)	
			(a) Sharp RD design			
Treatment effect	-0.497	-0.427	17.166	25.516	-0.149	-0.127
	(0.489)	(0.471)	(20.092)	(18.220)	(0.156)	(0.154)
Obs.	265	265	265	265	273	273
bw.	9.19	9.19	9.19	9.19	9.12	9.12
Obs. bw.	122	122	122	122	129	129
Department FE	Yes	Yes	Yes	Yes	Yes	Yes
Covariates	No	Yes	No	Yes	No	Yes
Bandwidth	Opt	Opt	Opt	Opt	Opt	Opt

Notes: Table reports local polynomial regression-discontinuity estimation with robust bias-corrected confidence intervals and inference procedures following Calonico et al. (2014).

Table A7: Results on employment:
Robustness using municipalities on the *Seuil du Poitou*

	(1)	(2)	(3)	(4)
	Employment count		Employment density	
	(a) Sharp RD design			
Treatment effect	-165.072	1.256	-25.270	37.678
	(352.015)	(399.653)	(136.932)	(149.985)
Obs.	265	265	273	273
bw.	9.19	9.19	9.12	9.12
Obs. bw.	122	122	129	129
Department FE	Yes	Yes	Yes	Yes
Covariates	No	Yes	No	Yes
Bandwidth	Opt	Opt	Opt	Opt

Notes: Table reports local polynomial regression-discontinuity estimation with robust bias-corrected confidence intervals and inference procedures following Calonico et al. (2014).

Table A8: Results on far-right vote share:
Robustness using municipalities on the *Seuil du Poitou*

	(1)	(2)	(3)
	(a) Sharp RD design		
Treatment effect (%p)	-0.174	-0.174	0.093
	(0.815)	(0.815)	(0.800)
Obs.	273	273	273
bw.	11.4	11.4	11.4
Obs. bw.	139	139	139
Department FE	No	Yes	Yes
Covariates	No	No	Yes
Bandwidth	Opt	Opt	Opt

Notes: Table reports local polynomial regression-discontinuity estimation with robust bias-corrected confidence intervals and inference procedures following Calonico et al. (2014). Formal robustness test to bandwidth choice is presented in Figure A13.

Table A9: Treatment effect on population density with alternative cutoffs

	(1)	(2)	(3)	(4)	(5)	(6)	(7)	(8)	(9)
	(a) Sharp RD design on average share of far-right vote								
Placebo cutoffs	-30km	-15km	-7km	-5km	Baseline	+5km	+7km	+15km	+30km
Treatment	0.093	-0.175	-0.051	0.085	0.304***	0.025	0.090	-0.053	-0.161
	(0.457)	(0.135)	(0.246)	(0.208)	(0.117)	(0.130)	(0.134)	(0.186)	(0.261)
Obs.	4,747	4,747	4,747	4,747	4,747	4,747	4,747	4,747	4,747
Bandwidth (km)	16.2	20.6	16	18.6	20.4	12.3	12.5	14.4	24.5
Obs. bw.	990	1,906	1,599	1,720	1,795	1,303	1,292	738	1,176

Notes: Table reports local polynomial regression-discontinuity estimation with robust bias-corrected confidence intervals and inference procedures following Calonico et al. (2014). he dependent variable is the 2015 population density in residents per km2. The unit of analysis is the municipality. Robust standard errors are included.

Table A10: Treatment effect on employment density with alternative cutoffs

	(1)	(2)	(3)	(4)	(5)	(6)	(7)	(8)	(9)
	(a) Sharp RD design on average share of far-right vote								
Placebo cutoffs	-30km	-15km	-7km	-5km	Baseline	+5km	+7km	+15km	+30km
Treatment	0.063	-0.059	0.007	0.035	0.130***	0.022	0.065	-0.064	-0.125
	(0.185)	(0.057)	(0.108)	(0.089)	(0.049)	(0.060)	(0.061)	(0.075)	(0.126)
Obs.	4,888	4,888	4,888	4,888	4,888	4,888	4,888	4,888	4,888
Bandwidth (km)	17.1	24.4	16.4	18.3	22.8	15.1	14.1	17	25
Obs. bw.	1,051	2,157	1,666	1,758	2,003	1,521	1,441	1,533	1,262

Notes: Table reports local polynomial regression-discontinuity estimation with robust bias-corrected confidence intervals and inference procedures following Calonico et al. (2014). The dependent variable is the 2015 employment density in residents per km2. The unit of analysis is the municipality. Robust standard errors are included.

Table A11: Treatment effect on far-right vote share with alternative cutoffs

	(1)	(2)	(3)	(4)	(5)	(6)	(7)	(8)	(9)
	(a) Sharp RD design on average share of far-right vote								
Placebo cutoffs	-30km	-15km	-7km	-5km	Baseline	+5km	+7km	+15km	+30km
Treatment	-0.323	-0.344	-0.179	-0.347	1.460***	0.579	0.321	-0.989	0.290
	(0.556)	(0.501)	(0.524)	(0.484)	(0.382)	(0.572)	(0.579)	(0.620)	(0.375)
Obs.	4,887	4,887	4,887	4,887	4,887	4,887	4,887	4,887	4,887
Bandwidth (km)	14.1	16.6	15.6	14.2	18.2	14.7	15.6	16.9	21.7
Obs. bw.	863	1,703	1,632	1,530	1,734	1,501	1,540	1,515	1,088

Notes: Table reports local polynomial regression-discontinuity estimation with robust bias-corrected confidence intervals and inference procedures following Calonico et al. (2014). The dependent variable is the average share of far-right vote across the 2002, 2007, 2012 and 2017 French presidential elections. The unit of analysis is the municipality. Robust standard errors are included.

Table A12: Average *Front National* vote share around the border (Presidential elections, 2002-2017)

	(1)	(2)	(3)	(4)	(5)
	(a) Sharp RD design				
Treatment effect (%p)	1.401***	1.082***	1.156***	0.804***	1.118**
	(0.374)	(0.357)	(0.350)	(0.274)	(0.447)
Obs.	4,887	4,887	4,887	4,887	4,887
Bandwidth (km)	18	18	18	35.9	8.99
Obs. bw.	1,714	1,714	1,714	2,750	1,202
Department FE	No	Yes	Yes	Yes	Yes
Covariates	No	No	Yes	Yes	Yes
Bandwidth	Opt	Opt	Opt	2 $\times$ Opt	0.5 $\times$ Opt

Notes: Table reports local polynomial regression-discontinuity estimation with robust bias-corrected confidence intervals and inference procedures following Calonico et al. (2014).

Table A13: TURNOUT AND NON-FAR RIGHT VOTE SHARES

	(1)	(2)	(3)	(4)
Outcome:	Voter turnout	Vote share for: Extreme left	Center left	Center right
Treatment effect (%p)	-0.124	-0.354*	-0.274	-0.795*
	(0.285)	(0.189)	(0.430)	(0.437)
Obs.	4,887	4,887	4,887	4,887
Bandwidth (km)	22.1	17.6	18	25.3
Obs. bw.	1,960	1,695	1,719	2,153
Department FE	Yes	Yes	Yes	Yes
Covariates	Yes	Yes	Yes	Yes
Bandwidth	Opt	Opt	Opt	Opt

Notes: Table reports local polynomial regression-discontinuity estimation with robust bias-corrected confidence intervals and inference procedures following Calonico et al. (2014). Data-driven regression-discontinuity plots are presented in Figure A9.

Table A14: Mechanization and the far right vote share over time (1965-2017): Department-level analysis

	(1)	(2)	(3)
Outcome:	Far-right vote share		
Share of cons. muns. (%)	0.099***	0.017***	0.086***
	(0.011)	(0.005)	(0.014)
Obs.	747	747	747
Year FE	No	Yes	Yes
Department FE	No	No	Yes

Notes: "Share of cons. muns." stands for the departmental share of consolidated municipalities (measured in %). Spatial units are French Departments (NUTS3). Years covered (i.e., years with a far-right party qualified for the first round of the presidential elections) are 1965, 1974, 1988, 1995, 2002, 2007, 2012 and 2017.

A.2 Figures

Figure A1: Schematic illustration of a land consolidation reform

(a) Before consolidation

(b) After consolidation

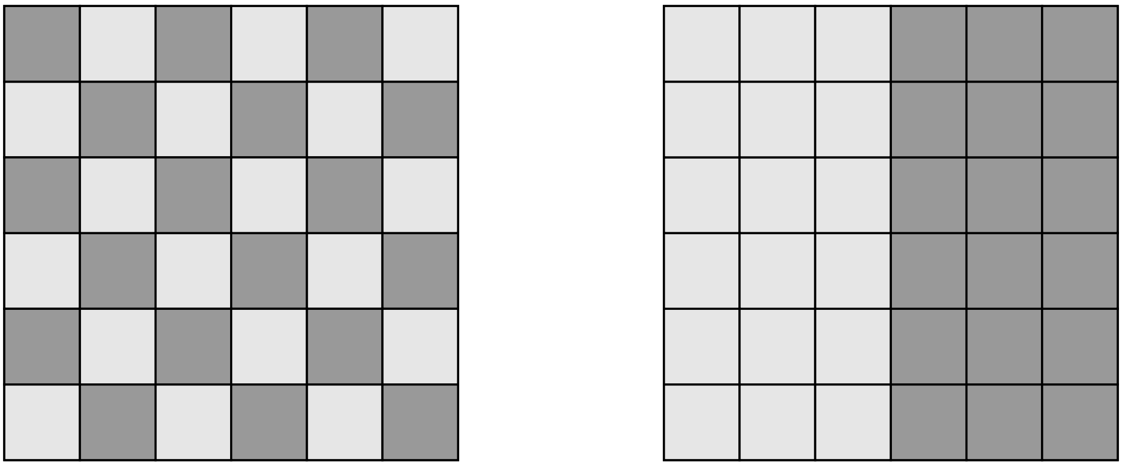

Figure A2: Map of consolidated municipalities in France (1945-2010)

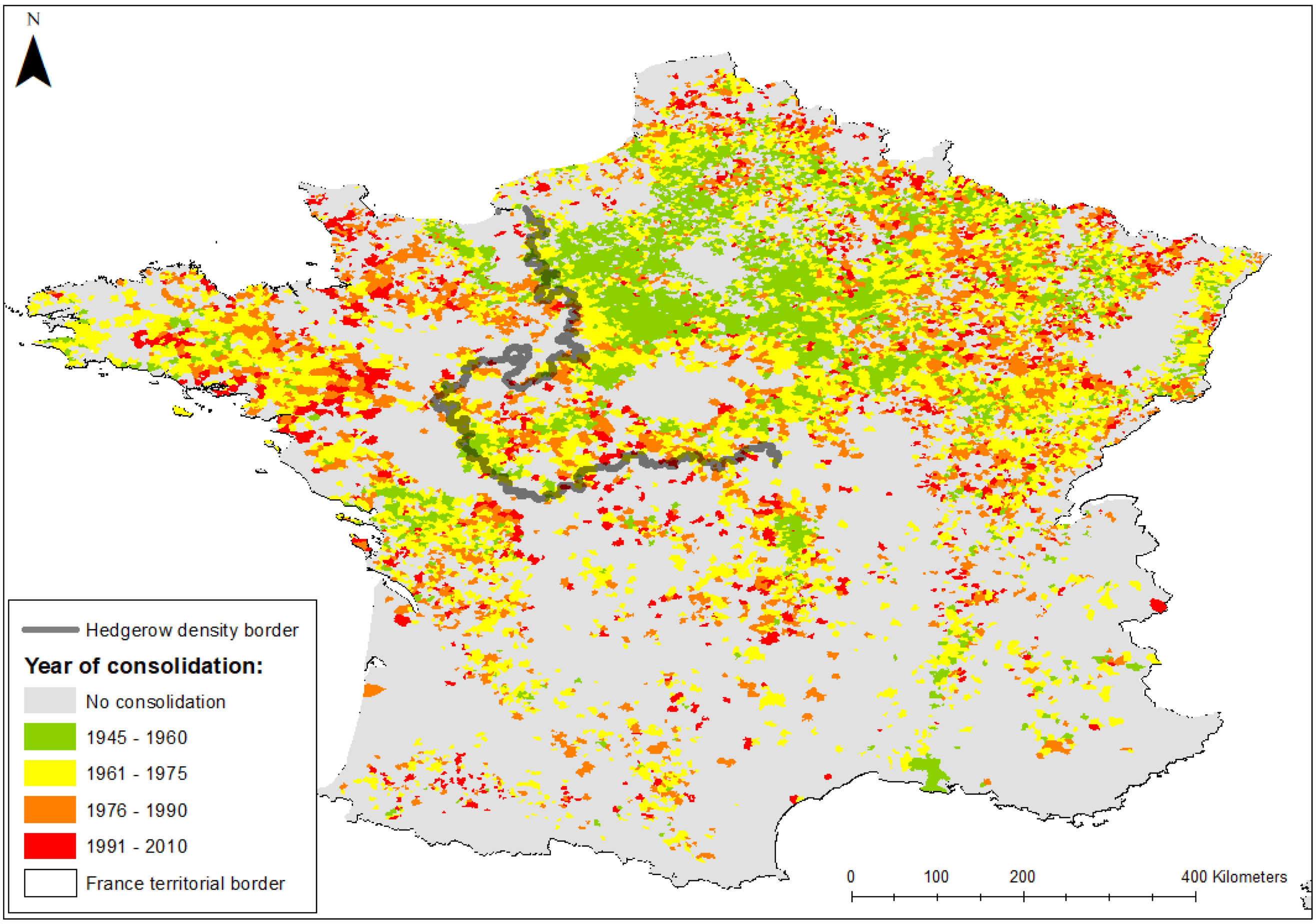

Source: Author's own illustration based on the land consolidation database by Philippe and Polombo (2013). By 2010, out of 36,766 municipalities in France, 15,498 (i.e., 42%) had consolidated their agricultural land.

Figure A3: France's soil composition

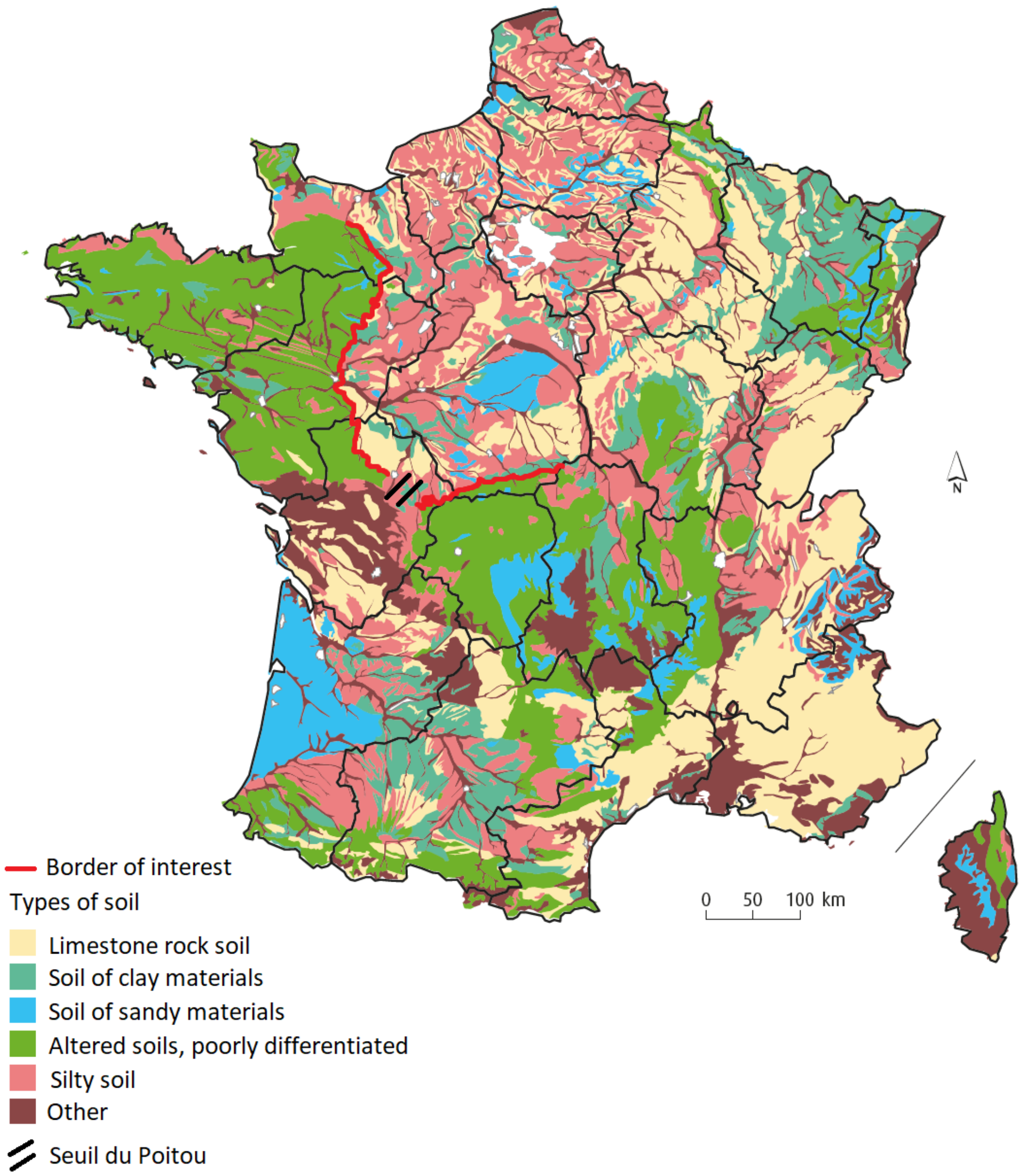

Notes: Author's own geo-referencing using ArcGIS. *Source:* Inra, BDGSF, Ministry of Ecology, Sustainable Development and Energy. Author's own translation. *Scale:* 1/1 000 000, 1998. *Processing*: SOeS, 2014.

Figure A4: Armorican and Central Massifs

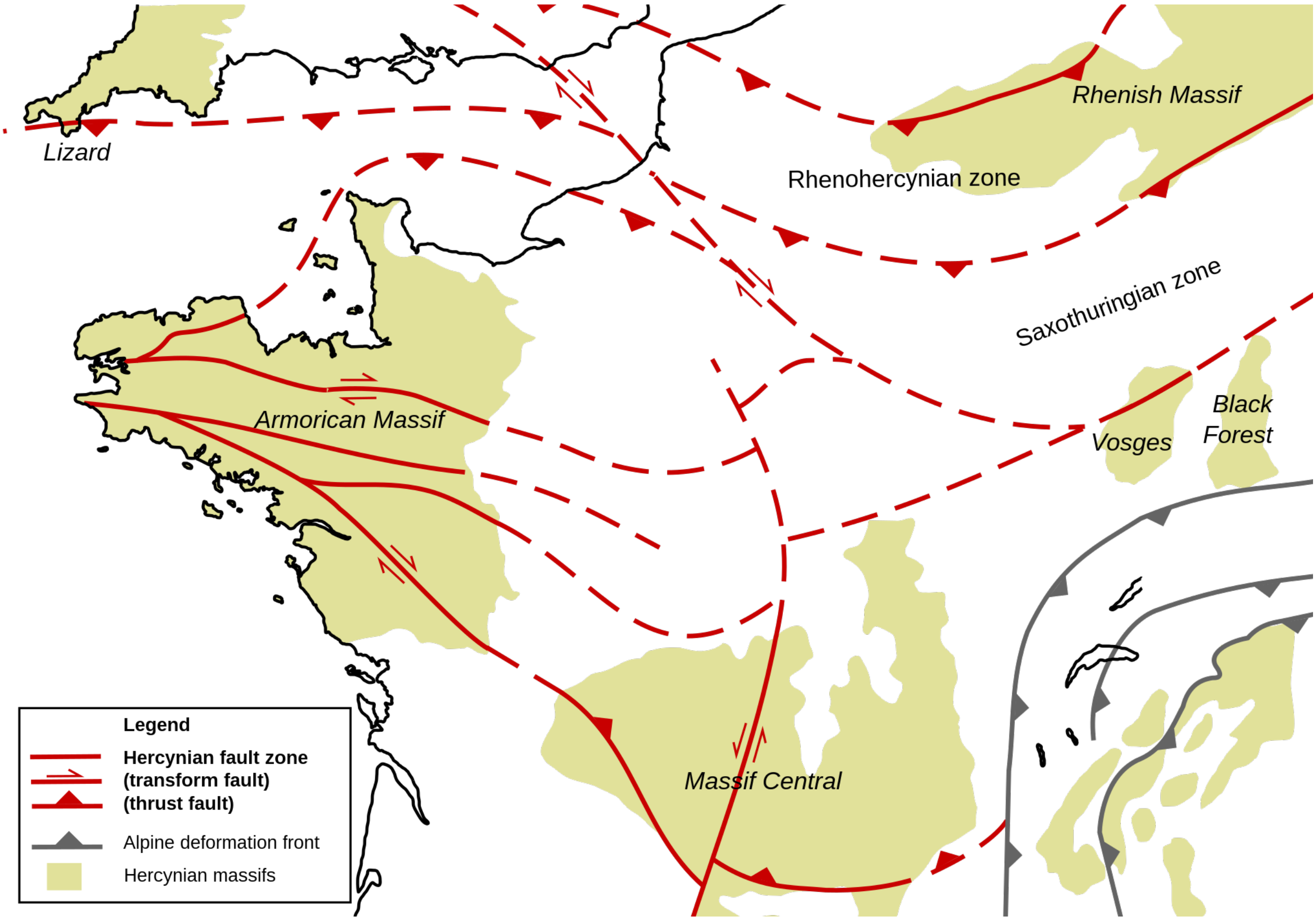

Figure A5: Elevation around the hedgerow density border

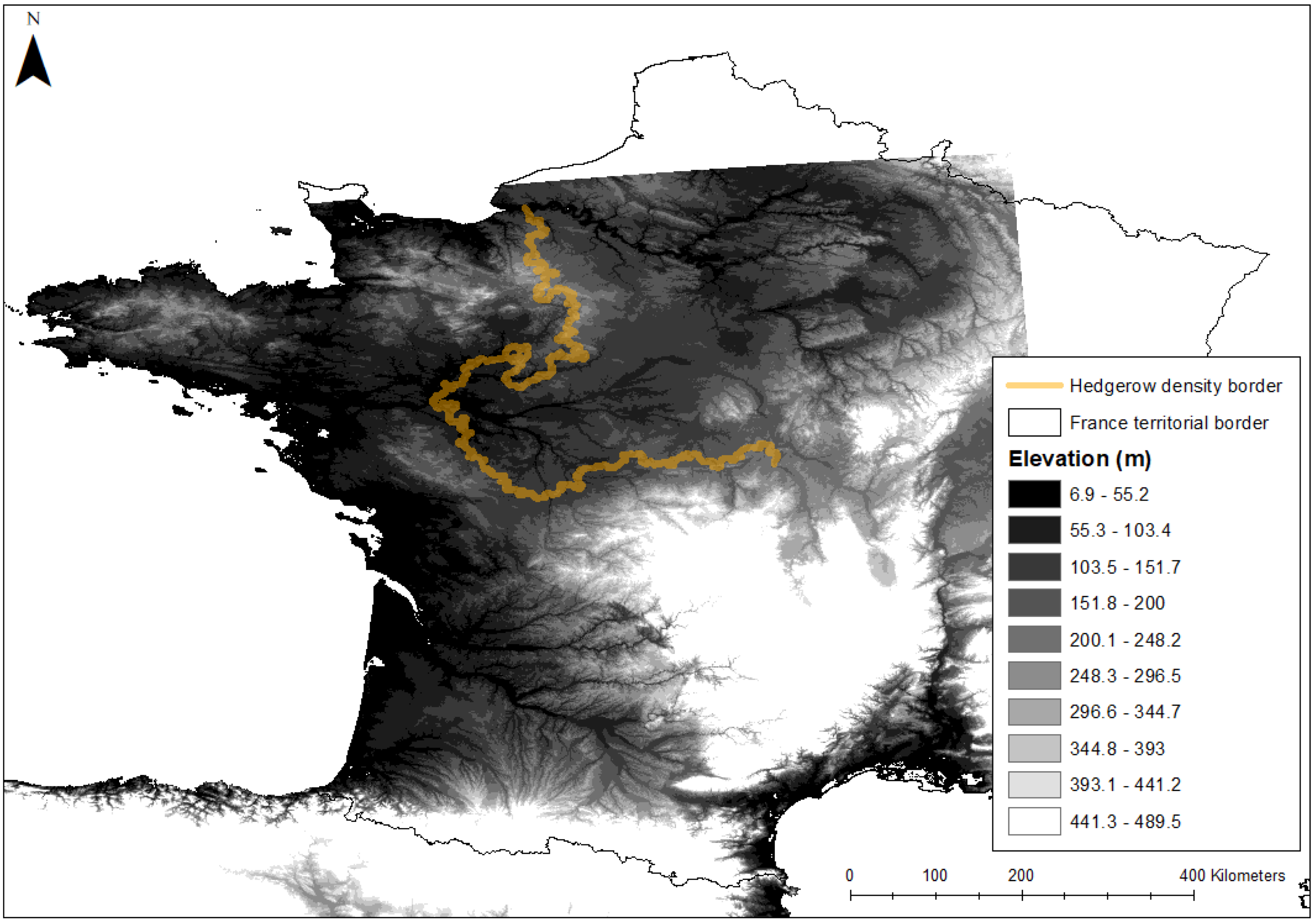

Source: Author's own illustration based the EU's 2018 layer of the Copernicus Land Monitoring Service (spatial resolution of 25m).

Figure A6: RD plot: Mechanization and long-term productivity

(a) Production per ha (€)

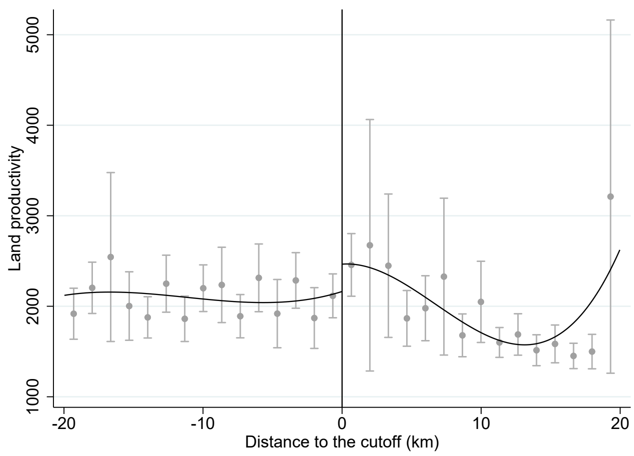

(b) Production per worker (€)

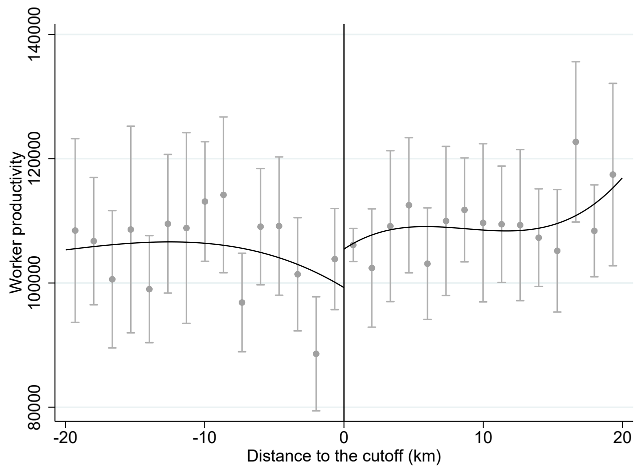

Notes: Data-driven regression-discontinuity plots following Calonico et al. (2014). 95% confidence intervals are presented.

Figure A7: RD PLOT: EMPLOYMENT DENSITY

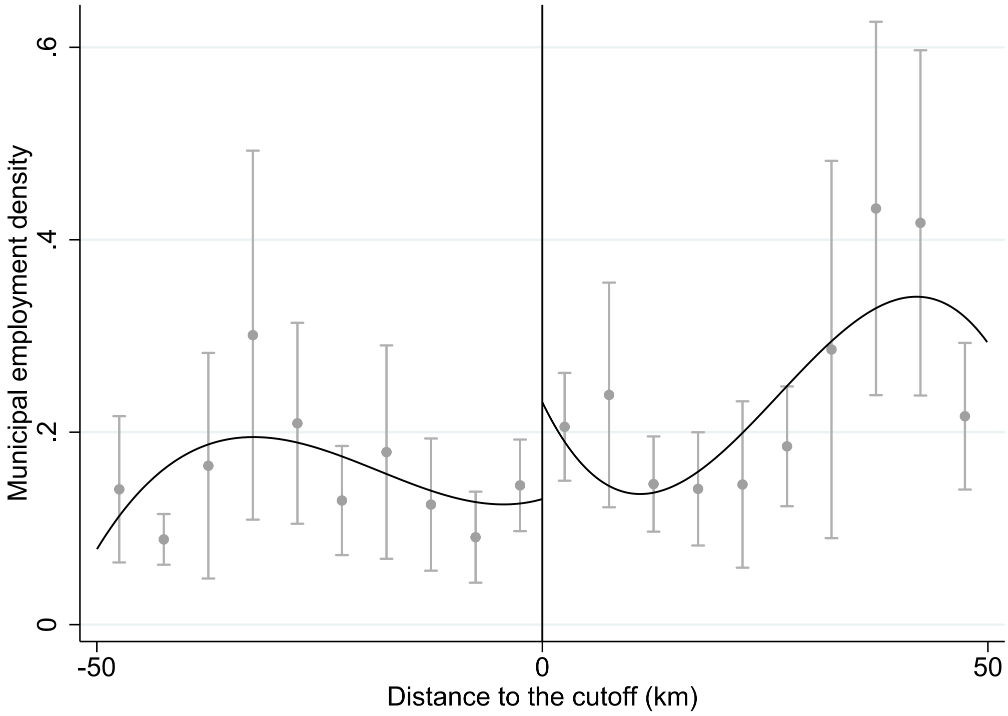

Notes: Data-driven regression-discontinuity plot following Calonico et al. (2014). 95% confidence intervals are presented.

Figure A8: Population around the threshold

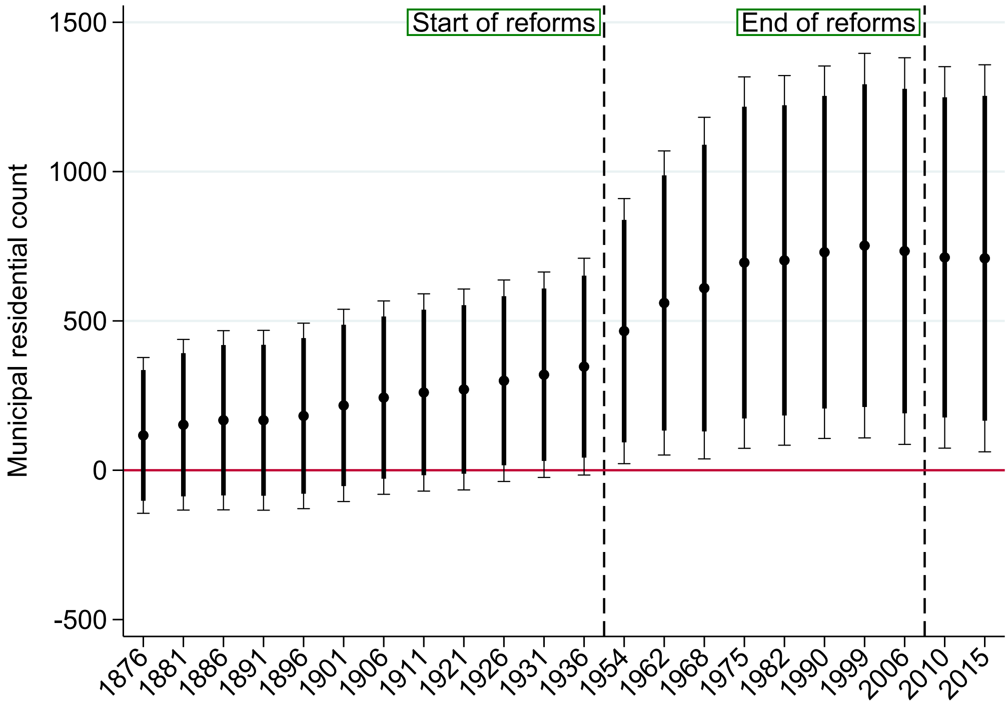

Notes: Figure reports local polynomial regression-discontinuity estimations with robust bias-corrected confidence intervals and inference procedures following Calonico et al. (2014). Regressions are conducted for each year separately between 1876 and 2015. The municipal residential count for each year is the outcome. Land consolidation reforms took place between 1945 and 2008 (cf. Figure 2).

Figure A9: Non-far-right voting shares and turnout around the cutoff (municipal level, 2002-2017)

(a) Voter turnout (%)

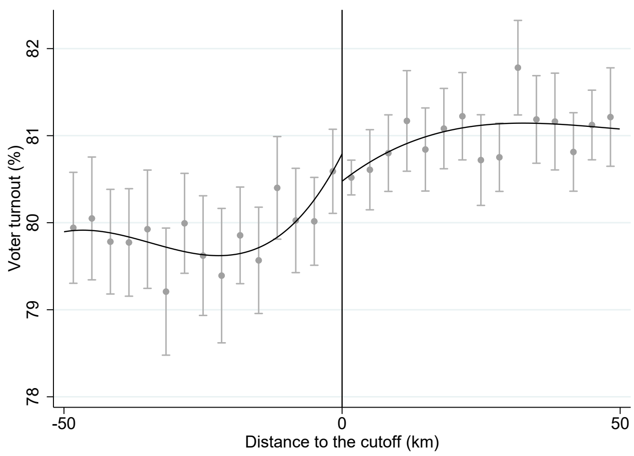

(b) Share of far-left votes (%)

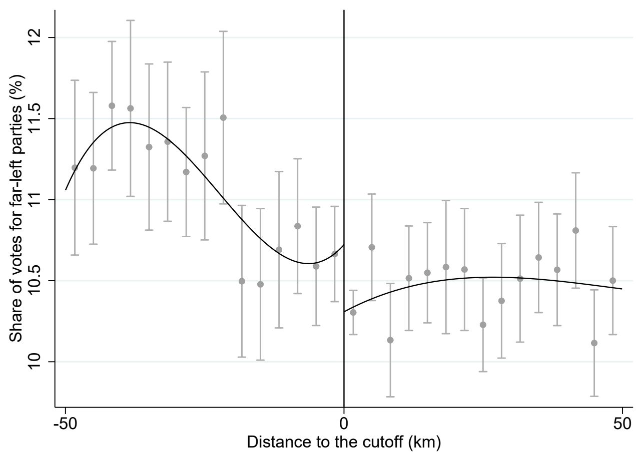

(c) Share of center left votes (%)

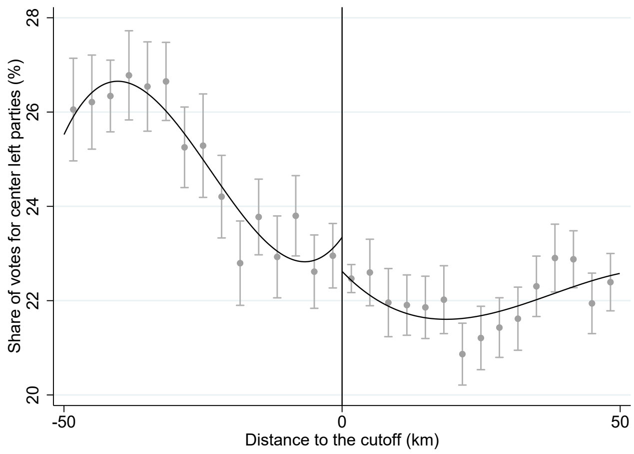

(d) Share of center right votes (%)

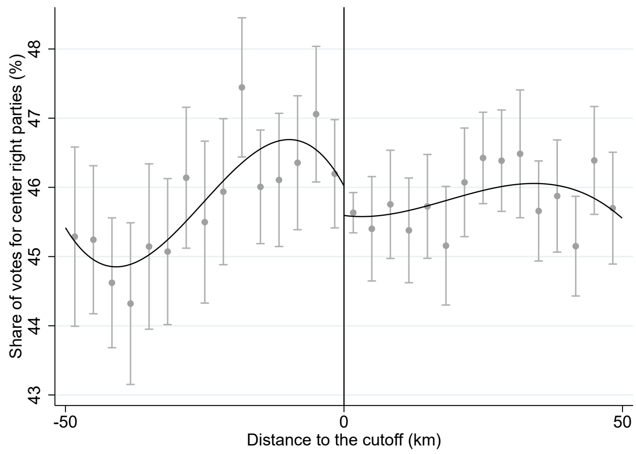

Notes: Data-driven regression-discontinuity plots following Calonico et al. (2014). 95% confidence intervals are presented. Local polynomial regression-discontinuity estimation with robust bias-corrected confidence intervals are presented in Table A13.

Figure A10: Placebo cutoffs

(a) RD plot with optimal cutoff + 1km

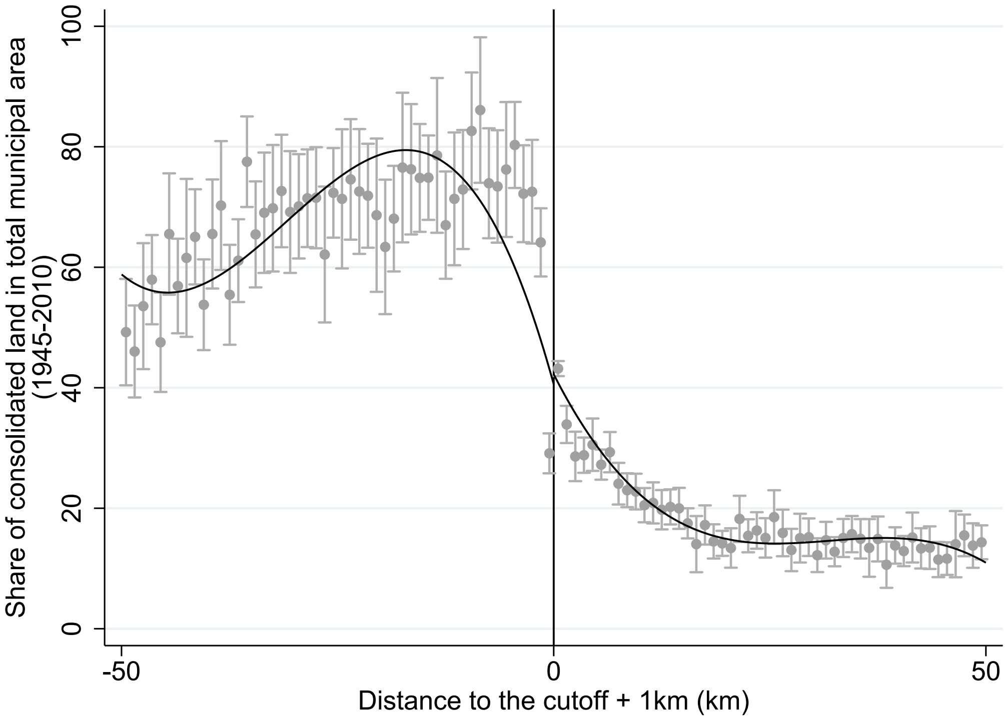

(b) RD plot with optimal cutoff - 1km

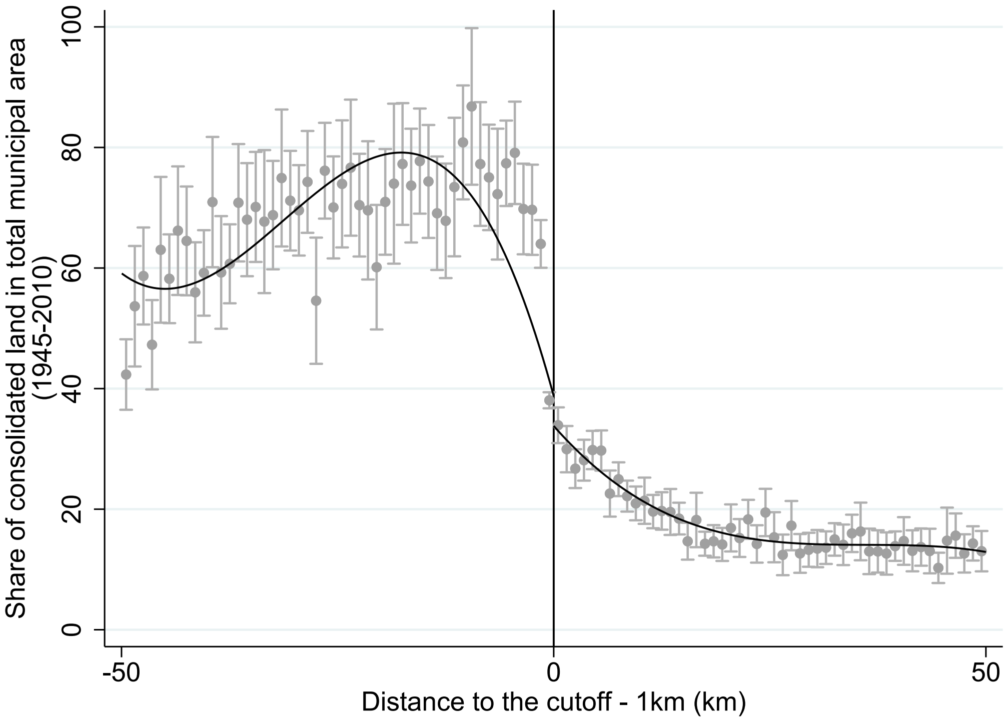

Notes: Data-driven regression-discontinuity plots following Calonico et al. (2014). 95% confidence intervals are presented. Threshold is artificially "shifted" by ±1km. Outcome is the share of consolidated land between 1945 and 2010.

Figure A11: Alternative bandwidth choices: Population density

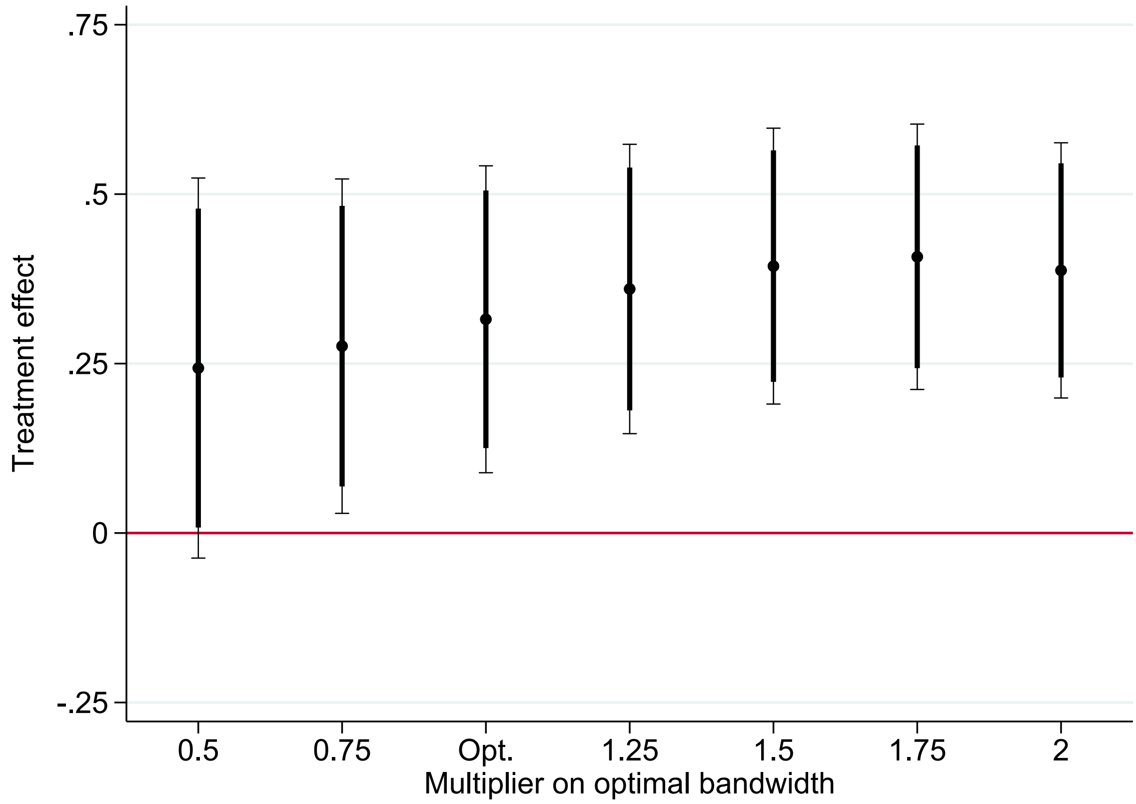

Notes: Figure reports local polynomial regression-discontinuity estimation following Calonico et al. (2014). Optimal bandwidth: 21.651km. The bandwidth size varies from 0.5 times the optimal bandwidth to 2 times the optimal bandwidth, with 0.25 increments. The dependent variable is 2010 population density in residents per km2. The unit of analysis is the municipality. Robust standard errors are included.

Figure A12: Alternative bandwidth choices: Employment density

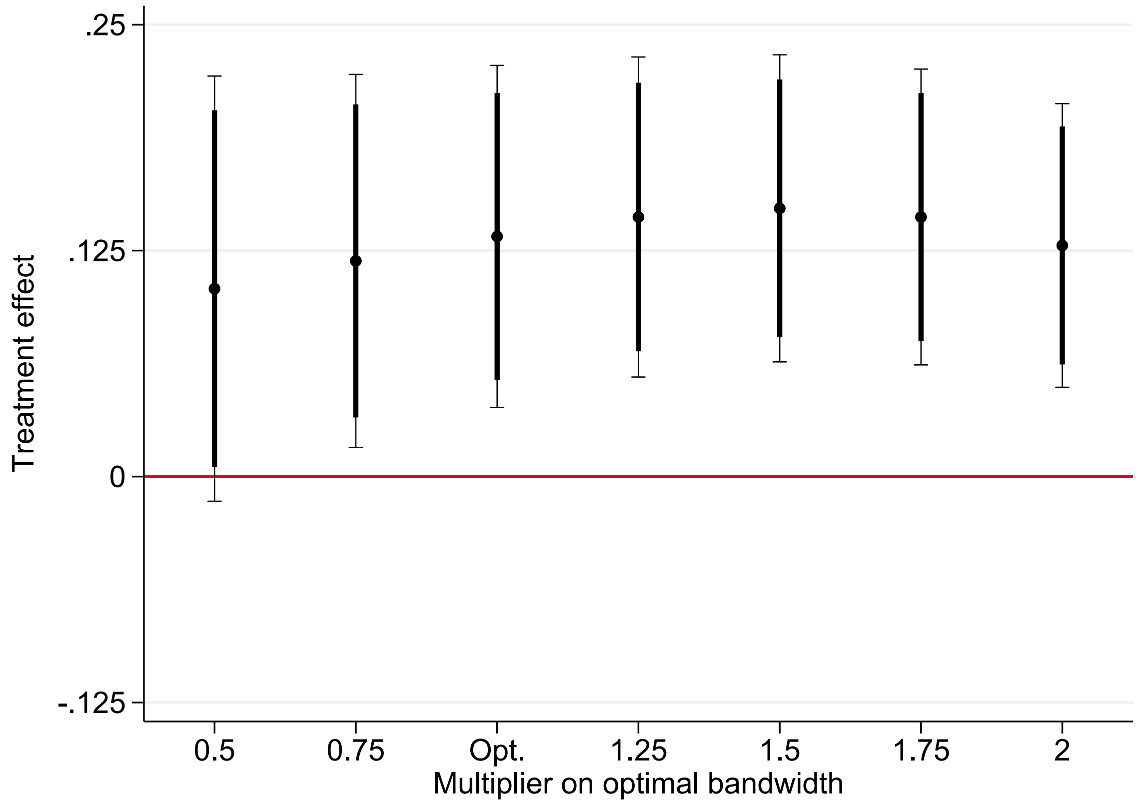

Notes: Figure reports local polynomial regression-discontinuity estimation following Calonico et al. (2014). Optimal bandwidth: 24.136km. The bandwidth size varies from 0.5 times the optimal bandwidth to 2 times the optimal bandwidth, with 0.25 increments. The dependent variable is the 2010 employment density (at the workplace) in workers per km2. The unit of analysis is the municipality. Robust standard errors are included.

Figure A13: Alternative bandwidth choices: Far-right vote share

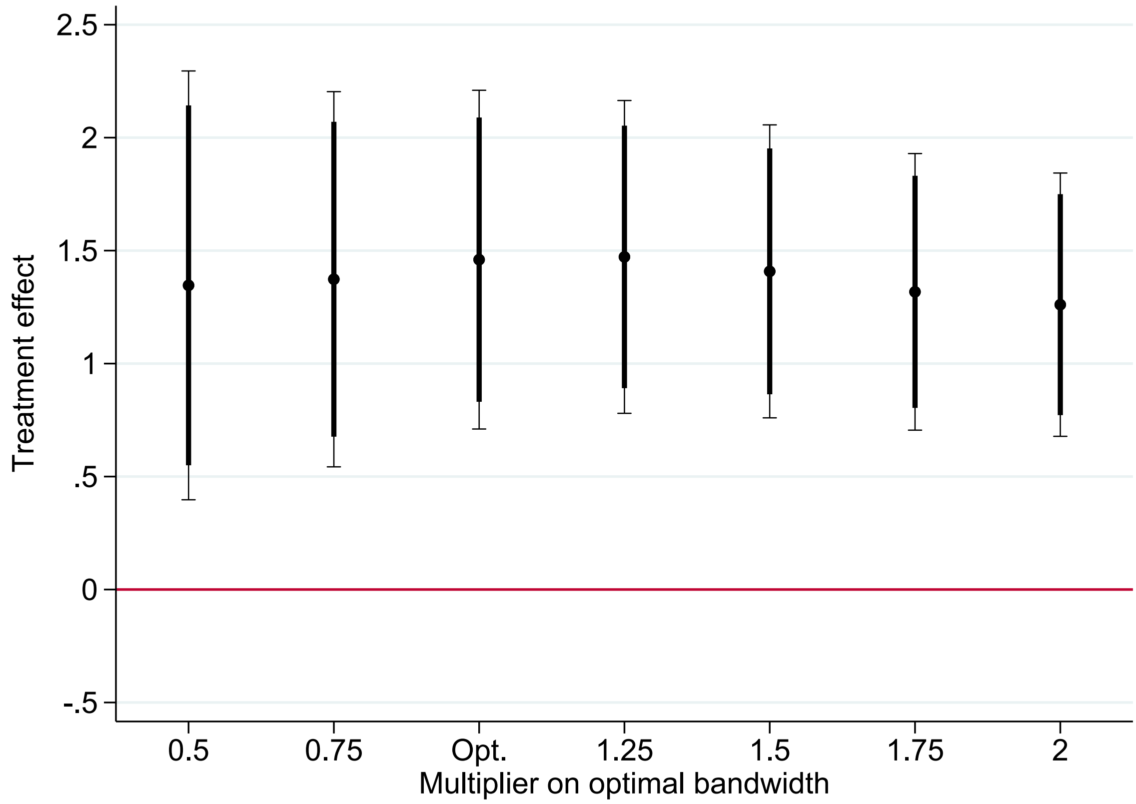

Notes: Figure reports local polynomial regression-discontinuity estimation following Calonico et al. (2014). Optimal bandwidth: 18.173km. The bandwidth size varies from 0.5 times the optimal bandwidth to 2 times the optimal bandwidth, with 0.25 increments. The dependent variable is the average share of far-right vote across the 2002, 2007, 2012 and 2017 French presidential elections. The unit of analysis is the municipality. Robust standard errors are included.

Figure A14: Land consolidation and far-right vote share (1965-2017)

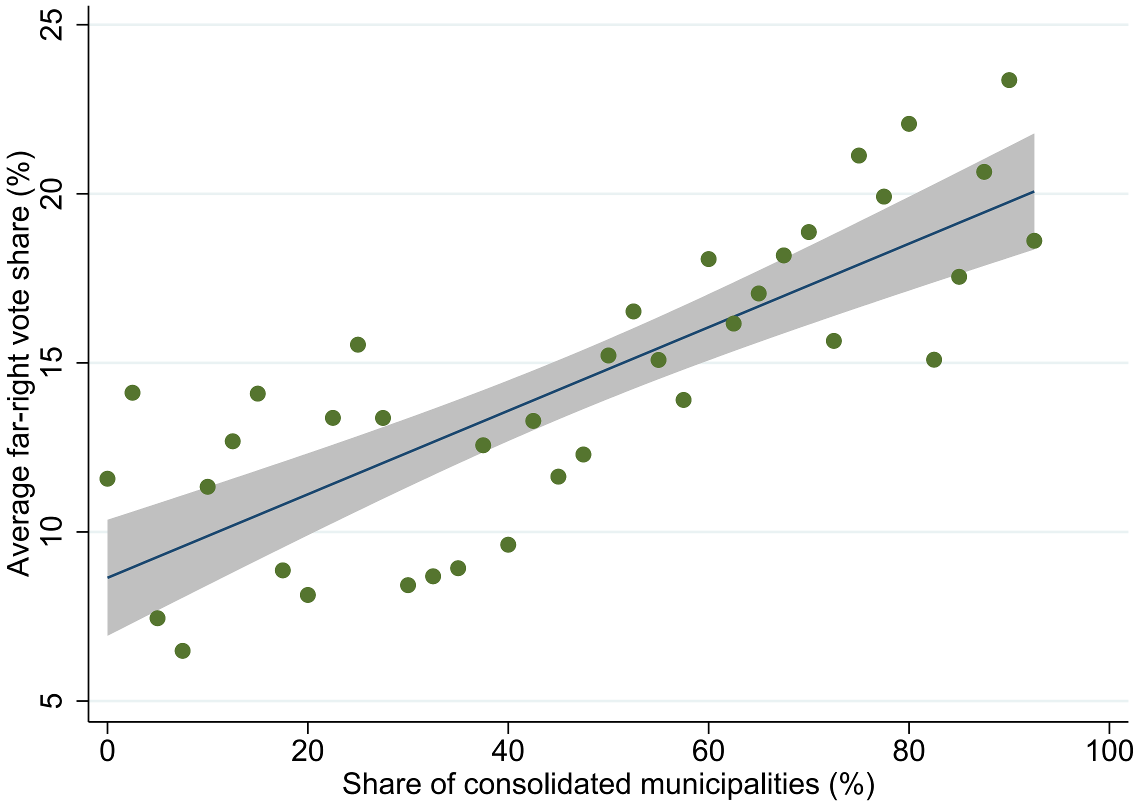

Notes: Spatial units are French Departments (NUTS3). Years covered (i.e., with a far right party qualified for the first round of the presidential elections) are 1965, 1974, 1988, 1995, 2002, 2007, 2012 and 2017. Average far-right vote share taken within 2.5%p bins in the share of consolidated municipalities. 95% confidence intervals are included.

Figure A15: Number and size of historical settlements

(Cassini map, 18th century)

(a) Number of historical settlements

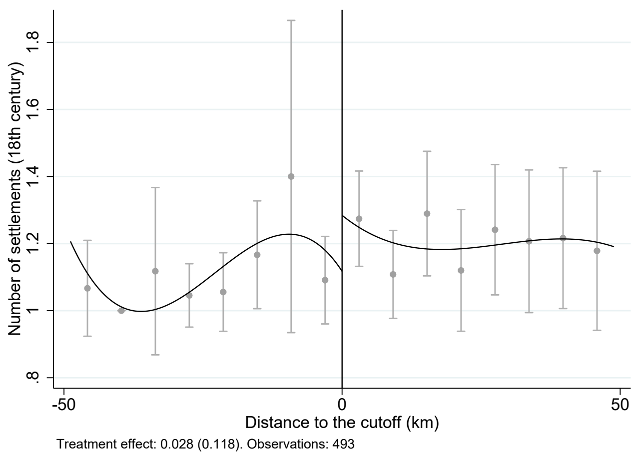

(b) Size of historical settlements

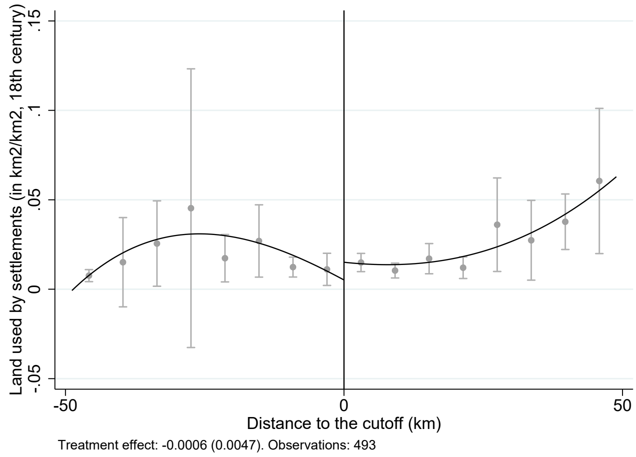

Notes: RD plot following Calonico et al. (2014).

Working Papers of the Center of Economic Research at ETH Zurich

(PDF-files of the Working Papers can be downloaded at www.cer.ethz.ch/research/working-papers.html).

21/376 G. Loumeau
Land Consolidation Reforms: A Natural Experiment on the Economic and Political Effects of Agricultural Mechanization

21/375 L. Bretschger
Green Road is Open: Economic Pathway with a Carbon Price Escalator

22/374 A. Goussebaïle
Democratic Climate Policies with Overlapping Generations

22/373 H. Gersbach, O. Tejada, J. Wagner
Policy Reforms and the Amount of Checks & Balances

22/372 S. Houde, W. Wang
The Incidence of the U.S.-China Solar Trade War

22/371 J. A. Bingler
Expect the worst, hope for the best: The valuation of climate risks and opportunities in sovereign bonds

22/370 A. Bommier, A. Fabre, A. GoussebaÃ¯le, and D. Heyen
Disagreement Aversion

22/369 A. Jo, A. Miftakhova
How Constant is Constant Elasticity of Substitution? Endogenous Substitution between Clean and Dirty Energy

22/368 N. Boogen, M. Filippini, A. L. Martinez-Cruz
Value of co-benefits from energy saving ventilation systems–Contingent valuations on Swiss home owners

22/367 D. Bounie, A. Dubus, P. Waelbroeck
Market for Information and Selling Mechanisms

22/366 N. Kumar, N. Kumar Raut, S. Srinivasan
Herd behavior in the choice of motorcycles: Evidence from Nepal

21/365 E. Komarov
Capital Flows and Endogenous Growth

21/364 L. Bretschger, A. Jo
Complementarity between labor and energy: A firm-level analysis

21/363 J. A. Bingler, C. Colesanti Senni, P. Monnin
Climate Transition Risk Metrics: Understanding Convergence and Divergence across Firms and Providers

21/362 S. Rausch, H. Yonezawa
Green Technology Policies versus Carbon Pricing: An Intergenerational Perspective

21/361 F. Landis, G. Fredriksson, S. Rausch
Between- and Within-Country Distributional Impacts from Harmonizing Carbon Prices in the EU

21/360 O. Kalsbach, S. Rausch
Pricing Carbon in a Multi-Sector Economy with Social Discounting

21/359 S. Houde, T. Wekhof
The Narrative of the Energy Efficiency Gap

21/358 F. Böser, H. Gersbach
Leverage Constraints and Bank Monitoring: Bank Regulation versus Monetary Policy

21/357 F. Böser
Monetary Policy under Subjective Beliefs of Banks: Optimal Central Bank Collateral Requirements

21/356 D. Cerruti, M. Filippini
Speed limits and vehicle accidents in built-up areas: The impact of 30 km/h zones

21/355 A. Miftakhova, C. Renoir
Economic Growth and Equity in Anticipation of Climate Policy

21/354 F. Böser, C. Colesanti Senni
CAROs: Climate Risk-Adjusted Refinancing Operations

21/353 M. Filippini, N. Kumar, S. Srinivasan
Behavioral Anomalies and Fuel Efficiency: Evidence from Motorcycles in Nepal

21/352 V. Angst, C. Colesanti Senni, M. Maibach, M. Peter, N. Reidt, R. van Nieuwkoop
Economic impacts of decarbonizing the Swiss passenger transport sector

21/351 N. Reidt
Climate Policies and Labor Markets in Developing Countries

21/350 V. Britz, H. Gersbach
Pendular Voting

21/349 E. Grieg
Public opinion and special interests in American environmental politics

21/348 N. Ritter, J. A. Bingler
Do homo sapiens know their prices? Insights on dysfunctional price mechanisms from a large field experiment

20/347 C. Daminato, M. Filippini, F. Haufler
Personalized Digital Information and Tax-favoured Retirement Savings: Quasi-experimental Evidence from Administrative Data

20/346 V. Britz, H. Gersbach
Open Rule Legislative Bargaining

20/345 A. Brausmann, E. Grieg
Resource Discoveries and the Political Survival of Dictators

20/344 A. Jo
The Elasticity of Substitution between Clean and Dirty Energy with Technological Bias

20/343 I. van den Bijgaart, D. Cerruti
The effect of information on market activity; evidence from vehicle recalls

20/342 H. Gersbach, R. Wattenhofer
A Minting Mold for the eFranc: A Policy Paper

20/341 L. Bretschger
Getting the Costs of Environmental Protection Right

20/340 J. A. Bingler, C. Colesanti Senni
Taming the Green Swan: How to improve climate-related financial risk assessments

20/339 M. Arvaniti, T. Sjögren
Temptation in Consumption and Optimal Redistributive Taxation

20/338 M. Filippini, S. Srinivasan
Voluntary adoption of environmental standards and limited attention: Evidence from the food and beverage industry in Vietnam

20/337 F. Böser, C. Colesanti Senni
Emission-based Interest Rates and the Transition to a Low-carbon Economy

20/336 L. Bretschger, E. Grieg, P. J.J. Welfens, T. Xiong
Corona Fatality Development and the Environment: Empirical Evidence for OECD Countries